

# Geological Survey of Finland

**Bulletin 278**

**Deformation analysis  
of a Precambrian mafic intrusive:  
Haukivesi area, Finland**

**by Jyrki Parkkinen**

**Geologinen tutkimuslaitos • Espoo 1975**



**Parkkinen, J. 1975:** Deformation analysis of a Precambrian mafic intrusive: Haukivesi area, Finland. *Geological Survey of Finland, Bulletin 278*, 61 pages, 44 figures, 4 tables.

The Joutsenmäki intrusive is an elongated body, 18 km long and a maximum of 6 km wide, composed of pyroxene diorite and gabbro. It is surrounded by supracrustal rocks metamorphosed under the conditions of the amphibolite facies. The fracture pattern in relation to the petrography of the intrusive, and the structure of the intrusive in relation to the structural patterns of its surroundings are studied using map data and statistical analysis of tectonic elements. Some aspects of the regional tectonics of eastern Finland are discussed.

The intrusion, in the form of a sill or laccolith, took place before the peak of regional metamorphism and major regional movements including faulting and associate folding of the supracrustal formations. During this post-intrusion phase, the mafic body suffered deformation and metamorphism concentrated in narrow zones.

*The author's address:*

*Jyrki Parkkinen  
Outokumpu Oy  
Exploration Department  
P.O. Box 27  
SF-02101 Espoo 10*

ISBN 951-690-031-3

Helsinki 1975. Valtion painatuskeskus

Geological Survey of Finland, Bulletin 278

DEFORMATION ANALYSIS  
OF A PRECAMBRIAN MAFIC INTRUSIVE:  
HAUKIVESI AREA, FINLAND

BY  
JYRKI PARKKINEN

WITH 44 FIGURES AND 4 TABLES IN THE TEXT

GEOLOGINEN TUTKIMUSLAITOS  
ESPOO 1975

## CONTENTS

	page
Introduction .....	5
Geological outline .....	7
Field and map data .....	15
Structural elements, their origin and relative ages .....	15
Outside the intrusive .....	15
Inside the intrusive .....	19
Lineament maps .....	21
Classification of foliation, fractures and lineaments .....	27
Structural interpretations .....	30
The intrusive .....	30
The southern Haukivesi area .....	34
The broader surroundings of the intrusive .....	34
Data treatment .....	39
Correction of field data .....	39
Structural diagrams .....	40
Regional trends of foliation, fractures and lineaments .....	41
Strain and stress analysis .....	41
Theoretical considerations .....	41
Practical consequences .....	45
Geological position and development of the intrusive .....	46
The location of the intrusive .....	46
The post-intrusion phase II .....	48
The post-intrusion phase I .....	49
The intrusion phase .....	50
The mechanism of intrusion .....	56
Conclusions .....	57
Acknowledgments .....	58
References .....	59

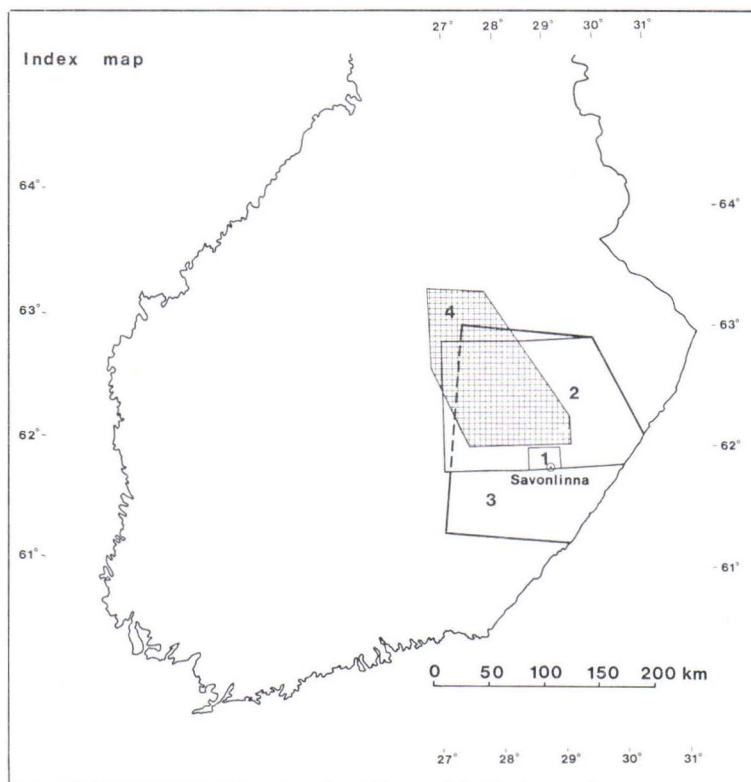


FIG. 1. Index map. 1. The southern Haukivesi area. 2. The area of a preliminary lineament study based on aerogeophysical maps (Fig. 31). 3. The broader surroundings of the intrusive (Savonlinna—Joensuu—Kuopio—Varkaus region). 4. The area studied by Talvitie, 1971 (Fig. 30).

## INTRODUCTION

The subject of this study is the structural geology of the southern Haukivesi area (Fig. 1) with particular emphasis on the Joutsenmäki mafic intrusive body. The work is a sequel to that carried out by the Exploration Department of Outokumpu Oy aiming at an elucidation of the geology of the Haukivesi area with its characteristic mafic and ultramafic plutonic rocks. The first report of this regional work, the petrological and structural analysis of the area, was given by Gaál and Rauhamäki (1971). In the present paper, special attention is paid to deformation by fracturing.

The Joutsenmäki mafic intrusive body is situated northwest of the town of Savonlinna (Figs. 1 and 2). It is an elongated body, 18 km long in a west-northwestern direction and a maximum of 6 km wide in a northern direction, composed of diorite and gabbro. For the sake of brevity this body will be called the intrusive in the following text.

Investigations dealing with the geology of the southern Haukivesi area have been published by Hackman (1933) and Gaál and Rauhamäki (1971). Saltikoff (1965) has described a trondhjemitic body northeast of the intrusive. Talvitie (1971) has investigated the geophysics and lineament tectonics of a region northwest of the intrusive. Gaál (1972) has discussed the tectonics of the Kotalahti Nickel Belt, which contains the Joutsenmäki intrusive. Korsman (1973) has compiled the Rantasalmi map sheet 3233 on a scale of 1:100 000; it adjoins map sheet area 4211, which contains the intrusive.

The petrographical description of the area is based (1) on the microscopical examination done by the author at the University of Helsinki, and (2) on the field work, microscopy and microprobe analyses carried out by the staff of Outokumpu Oy (Gaál and Rauhamäki, 1971; Parkkinen, 1971).

The main problems are, first, to relate the fracture pattern to the petrography of the intrusive, second, to relate the fracture pattern of the intrusive to the structural patterns of its surroundings, and third, to assess the information on the geological history of the intrusive that can be gained by fracture analytics.

Map analysis and statistical methods were employed. The map analysis includes the presentation of structural data on various types of maps by lineament techniques. The analyses are based on the structural data collected in the field and on the data interpreted from a variety of maps, including topographic maps, stereo-pair airphotos, lake maps, and gravimetric maps by the Finnish Geodetic Institute. In addition, maps of the Quaternary deposits and aeromagnetic and aereoelectric maps by the Geological Survey of Finland were used.

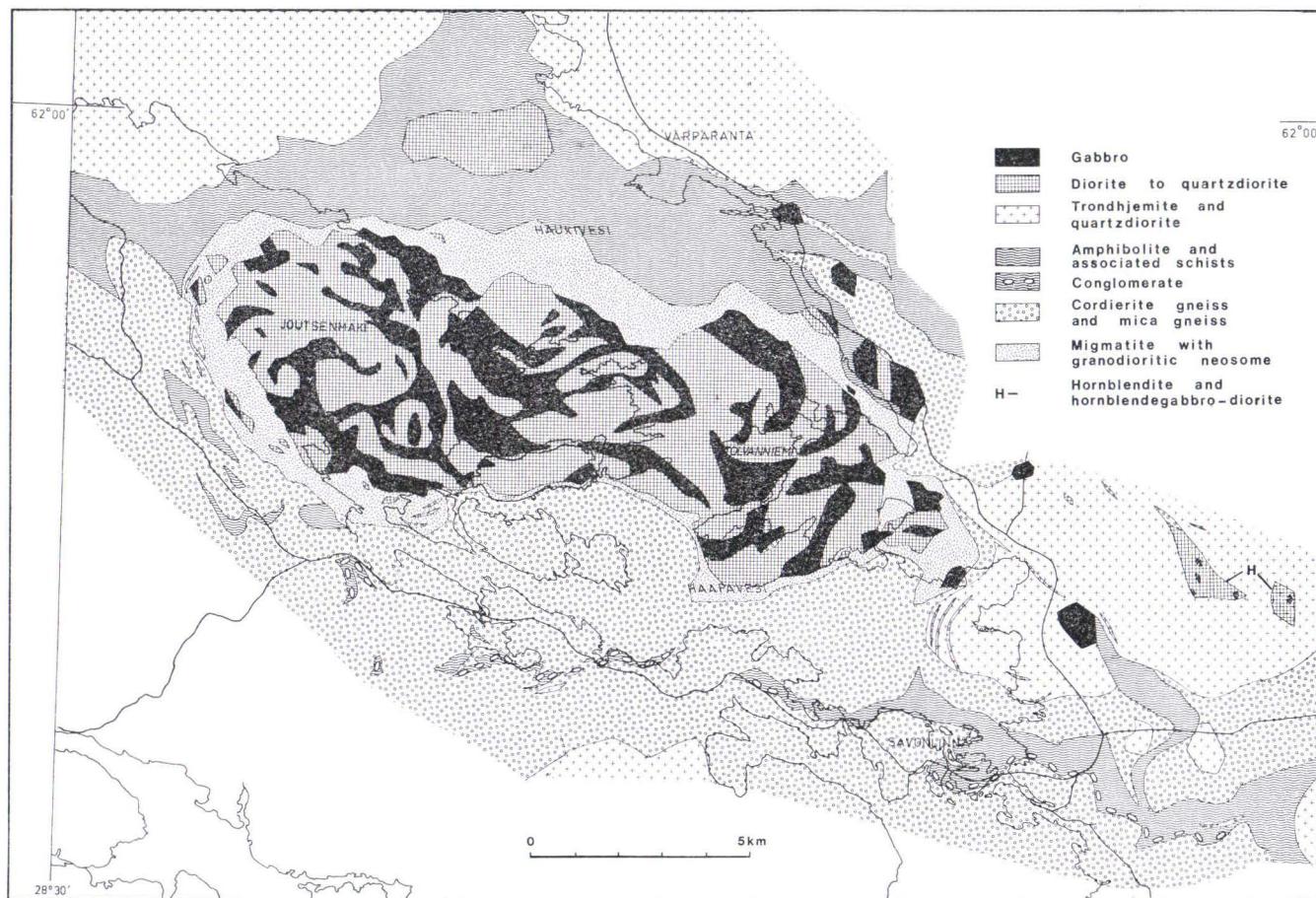


FIG. 2. A simplified petrographic map of the southern Haukivesi area.

The data treatment is based largely on the structural data collected in the field: the measured attitudes of 14 500 fractures, 4 033 foliation planes and 1 165 lineations. These data were gathered by the author and several other summer assistants during the mapping programme of Outokumpu Oy 1964—1970 under the leadership of E. Viluksela.

The main area of the study, including the intrusive and its close vicinity, will be called the southern Haukivesi area (Fig. 1). Out of the intrusive, a small portion has been investigated in detail. It will be called the Pyörlahti area (Fig. 20). Later on, the area of the lineament study was broadened to the Savonlinna—Joensuu—Kuopio—Varkaus region (Fig. 1) which is composed mainly of the more or less migmatized Svecokarelian schists and intrusives.

Unless otherwise stated, the nomenclature is adopted from the Glossary of Geology published by the American Geological Institute in 1972.

## GEOLOGICAL OUTLINE

The petrography of the southern Haukivesi area is simplified in Fig. 2. The intrusive is surrounded by a migmatite zone zero to 1.4 km broad containing fragments of the intrusive and relics of supracrustal rocks in a coarse porphyric granodioritic matrix. Adjacent to the migmatite zone there are amphibolites, conglomerate gneisses, and cordierite gneisses. Small mafic bodies and trondhjemitic to granodioritic rocks are located farther away and without any contact with the intrusive.

The intrusive is composed of medium-grained, equigranular pyroxene diorite with gabbroic portions. The primary constituents are plagioclase ( $An_{30-80}$ ), pyroxenes (bronzite and augite), and locally olivine, or, occasionally, hornblende and biotite. The boundaries between these rock types are largely transitional, in places sharp. The third major rock type is a feldspar porphyric diorite that has no observed connection with the above granodiorite. This rock type grades into the diorite or brecciates it and the gabbro of the intrusive (Figs. 3—5 and 8). On the maps, it is not distinguished from the even-grained diorite.

Minor rock types of the intrusive include mafic, felsic and composite dykes, mylonites, inclusions of supracrustal rocks, small bodies of sulphide ore, and mafic, fine-grained inclusions of diabase, plagioclase porphyrite and basalt-like rocks, possibly hornfelses or relics of the first crystalline portions of the intrusive (Figs. 4—5 and 8—11). The fine-grained inclusions seem to be rather evenly distributed, thus possibly indicating the vicinity of an intrusive contact throughout the exposed area. Close to the southern border of the intrusive, diorite and gabbro fragments are met with in a diorite and gabbro matrix (Fig. 12).





FIG. 3. A sharp contact between equigranular diorite and a banded and foliated mixture of diorite and feldspar porphyric diorite. The banding possibly originates from a flow structure. A thin pegmatite dyke and a few shear fractures with alteration zones around them.

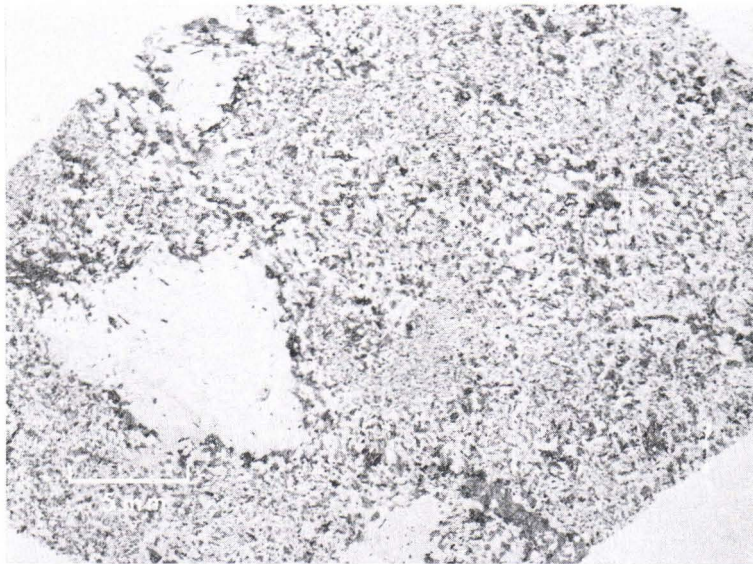


FIG. 4. A microphoto of a specimen with two rock types: fine-grained, basalt-like portions in equigranular, subophitic gabbro matrix. Some plagioclase grains appear to have grown at the expense of certain older products of the crystallization. In the biggest porphyroblasts there are relics of pyroxene-rich streaks. The porphyroblasts have grown in a contact of gabbro with porphyric diorite.

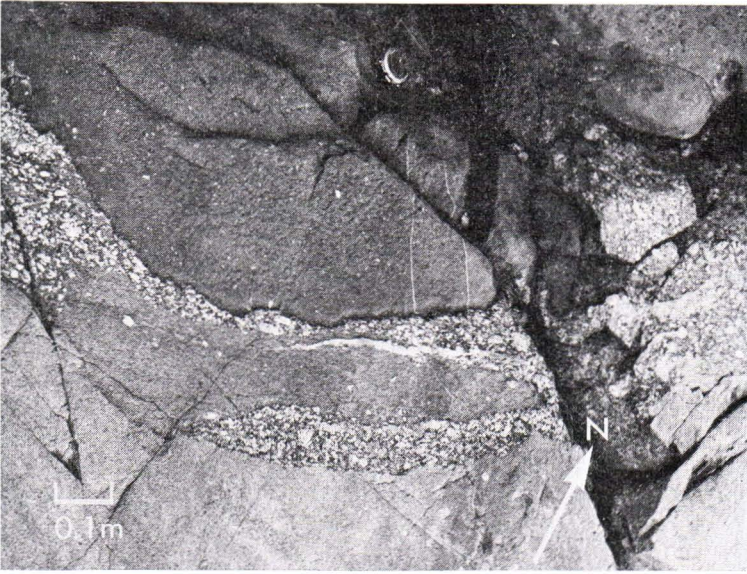


FIG. 5. Three rock types of the intrusive: fine-grained plagioclase porphyrite-like gabbro as inclusions with soft margins in equigranular diorite. In the contact zone and in some fractures porphyritic diorite brecciates the other rock types. A couple of very thin pegmatite dykes and some joints are seen in the gabbro.



FIG. 6. Pyroxene gabbro of the intrusive. A shear fracture dipping gently southwest is intersected by steeply dipping fractures striking  $335^{\circ}$  and  $035^{\circ}$ . A few steeply dipping joints striking north. A curved shear fracture dipping steeply north — northwest.

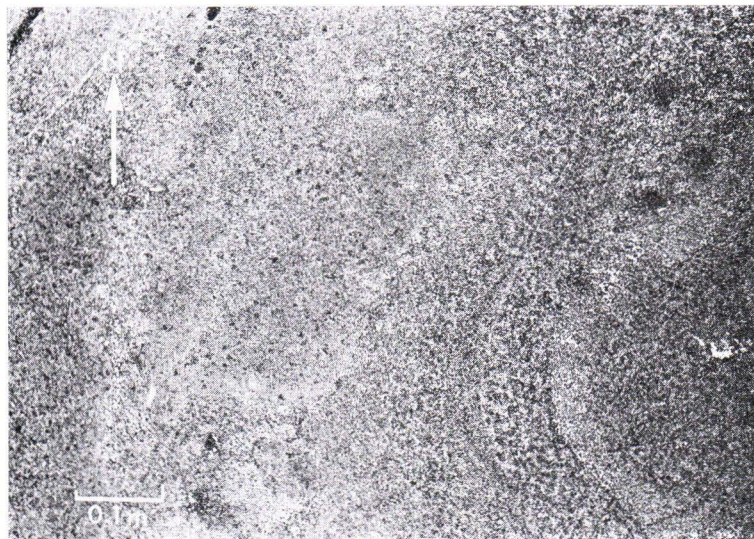


FIG. 7. Pyroxene diorite with fine- and coarser-grained streaks and weak foliation; a possible magmatic flow structure.

The major rock types of the intrusive have undergone a low-pressure metamorphism of the amphibolite to greenschist facies (*cf.* Hietanen, 1967; Miyashiro, 1973), or of the medium to low stage (*cf.* Winkler, 1970), which has produced relatively narrow zones (Fig. 26 B) of mineral assemblages containing actinolite, green hornblende, chlorite, epidote, biotite, and quartz.

The presence of pyroxene (bronzite and augite) suggests that the mafic inclusions and some of the mylonites and mafic dykes were formed under conditions similar to the high stage metamorphism or the pyroxene hornfels facies (Turner and Verhoogen, 1960). The absence of pyroxene and the presence of the plagioclase—quartz—biotite association indicates that some of the mafic dykes, most of the mylonites and most or all of the pegmatites crystallized under P-T conditions comparable to the amphibolite facies or medium-stage metamorphism. Moreover, a dark alteration zone from 1 to 50 cm broad generally exists around felsic dykes, shear fractures and mylonites. The alteration is similar to that of the major components mentioned above, being however more restricted and local (Figs. 3 and 6). It may be defined as local hydrothermal metamorphism (Miyashiro, 1973), which took place simultaneously with the fracturing of the intrusive.

The migmatite zone displays transitions from cordierite gneiss to coarse porphyric homogeneous granodiorite and, closest to the contact of the intrusive, to intensely foliated banded granodioritic cataclastic rock, augen gneiss (Figs. 13—15). There are also porphyric granodiorite veins in the supracrustal rocks in the vicinity of the migmatite zone. In the contact area, coarse porphyric granodiorite sends veins into and brecciates the rocks of the intrusive. Owing to the intense deformation,



FIG. 8. A mafic dyke in gabbro. The dyke displays relics of streaky, foliated porphyric diorite in sharp contact with the foliated gabbro. Another generation of foliation has been created in the dyke and in some of the fragments of the bedrock. The mafic dyke seems to have been foliated simultaneously with a right lateral fault movement. Observe the oblique foliation in the dyke and the drag features in the foliated bedrock to the left of the dyke.



FIG. 9. A composite dyke with two main components: fine-grained biotite diorite (dark) and coarser-grained quartzdiorite (light). The dyke is foliated except for some inner parts of the light streaks, which seem to have crystallized after the movements in the dyke. The light streaks roughly follow the intensive folding of the dark rock component. The plunge of the fold axes and mullions is almost vertical.



FIG. 10. A crush zone in gabbro with joints, shear fractures and mylonitic portions, and dipping gently south.

there are only a few relics of the possible contact reactions between the intrusive and granodiorite; viz. foliated gabbro and diorite with amphibole and biotite as the main dark minerals. The crystallization of the granodioritic neosome apparently occurred after the recrystallization of the supracrustal rocks and the crystallization of the intrusive. Hence, the supposed intrusive contact zone between the mafic body and the supracrustal rocks has been completely reworked by metamorphism.

According to Gaál and Rauhamäki (1971), the schists and gneisses around the intrusive derive from synorogenic miogeosynclinal facies turbidites deposited on eugeosynclinal volcanics. Conglomerate intercalations are found at the bottom of the turbidites. Owing to the metamorphism of the granulite facies, the turbidites have been converted into cordierite gneisses and the volcanics into amphibolites and diopside-amphibolites. The migmatization of the supracrustal rocks around the intrusives is connected with the mangeritic intrusives, the Joutsenmäki mafic body included.

In the present author's opinion, the forementioned grade of regional metamorphism is questionable. The mineral compositions presented by Gaál and Rauhamäki (Tables 1 and 2) are better suited to the low pressure metamorphism of the amphibolite facies (Hietanen, 1967; Miyashiro, 1973). With the exception of the narrow migmatite

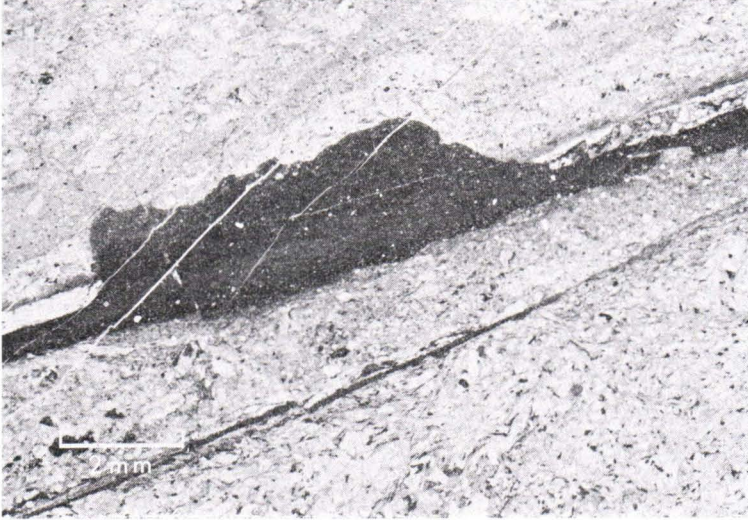


FIG. 11. Mylonitised gabbro: a transition from cataclastic mush to banded mylonite with a very fine-grained ultramylonitic band in the middle of the picture. The band has a fine laminated structure with microfolding, possibly a structure produced by ductile flow.



FIG. 12. Intrusive breccia close to the southern contact of the Joutsenmäki mafic body: dioritic (light) and gabbroic (dark) fragments in gabbroic matrix.



FIG. 13. Cordierite gneiss in which bedding cleavage is totally and schistosity ( $S_2$ ) partly destroyed by a younger foliation, crenulation cleavage ( $S_4$ ).



FIG. 14. Cordierite gneiss (A) grades to coarse porphyric granodiorite (B), which also brecciates it. A mafic dyke (C) cuts the migmatite parallel to the crenulation cleavage and minor strike slip faults. The contact zone of the dyke is weathered owing to abundant fine-grained biotite.



FIG. 15. Banded migmatite from the zone surrounding the intrusive. The migmatite grades to porphyric granodiorite on the one hand and to cordierite gneiss on the other. The texture of the rock is cataclastic, and the plagioclase augens seem to be syntectonically crystallized. This migmatite may be a blastomylonitic variant of cordierite gneiss.

zone around the intrusive, the supracrustal rocks are weakly migmatized. Medium-grained trondhjemitic and granitic stripes and veins, as well as transitional contacts of cordierite gneiss with a rock of trondhjemitic composition, occur in places both conform to and crossing the bedding or the foliation of the country rock.

The obvious lack of typically intrusive contact phenomena, such as chilled margins of the intrusive, dykes from the intrusive to the surrounding rocks, and thermoeffects of the intrusive to the surrounding metamorphic rocks and the inclusions mentioned above, are not consistent with the timing of the intrusion by Gaál and Rauhamäki (1971). The fine-grained inclusions and the breccias of the southern margin of the mafic body and, possibly, the petrographical zoning inside the body, are in agreement with the conclusion of Häkli (1971) that the intrusion took place in several phases.

## FIELD AND MAP DATA

### Structural elements, their origin and relative ages

#### Outside the intrusive

The lineations are minor fold axes and lineations of fabric elements (Fig. 36, diagrams 1, 3, 5 and 6). They are marked by the same symbol on the lineation map (Fig. 16,) because no conspicuous differences have been recognized between the plunges



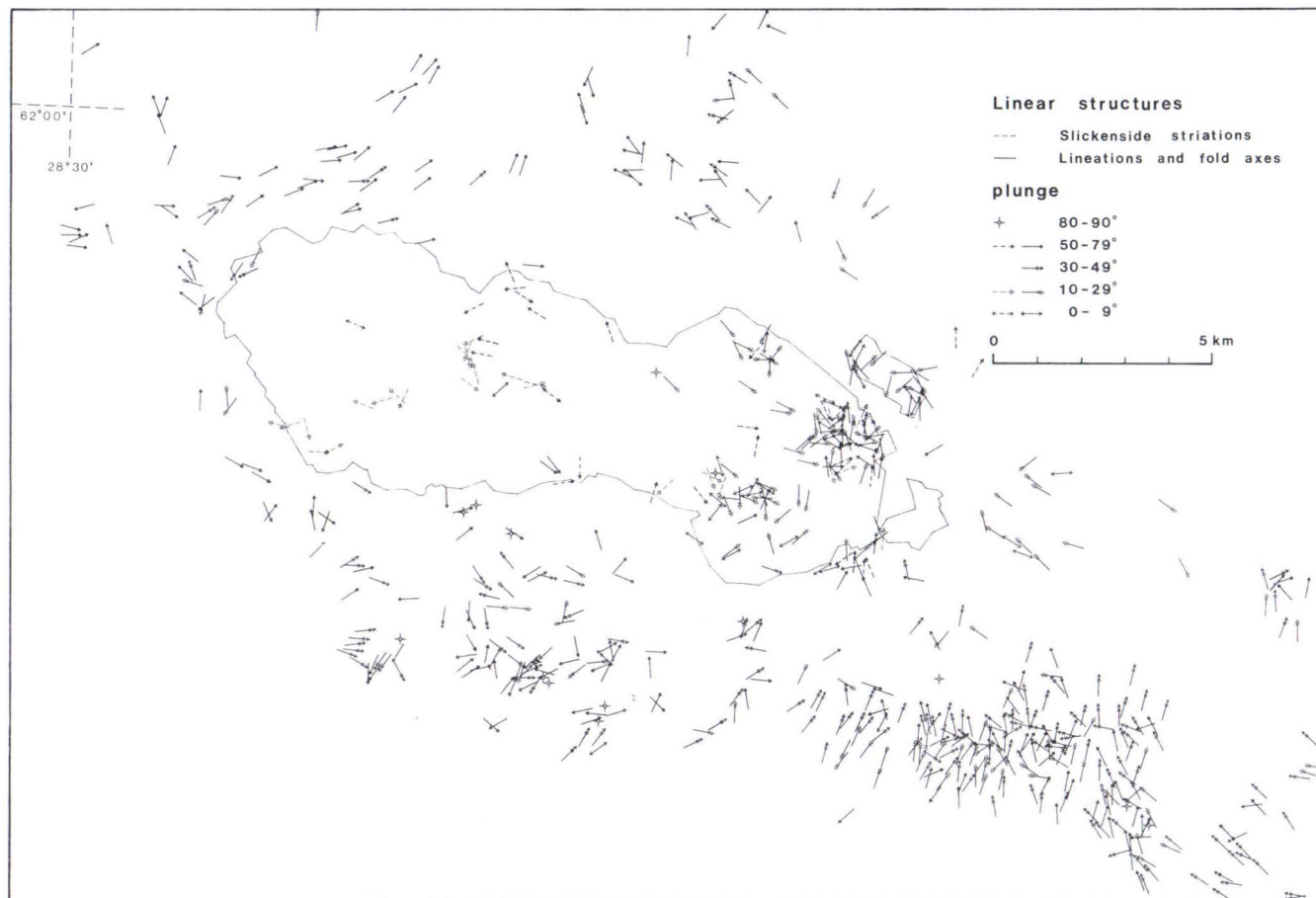


FIG. 16. Minor linear structures of the southern Haukivesi area.

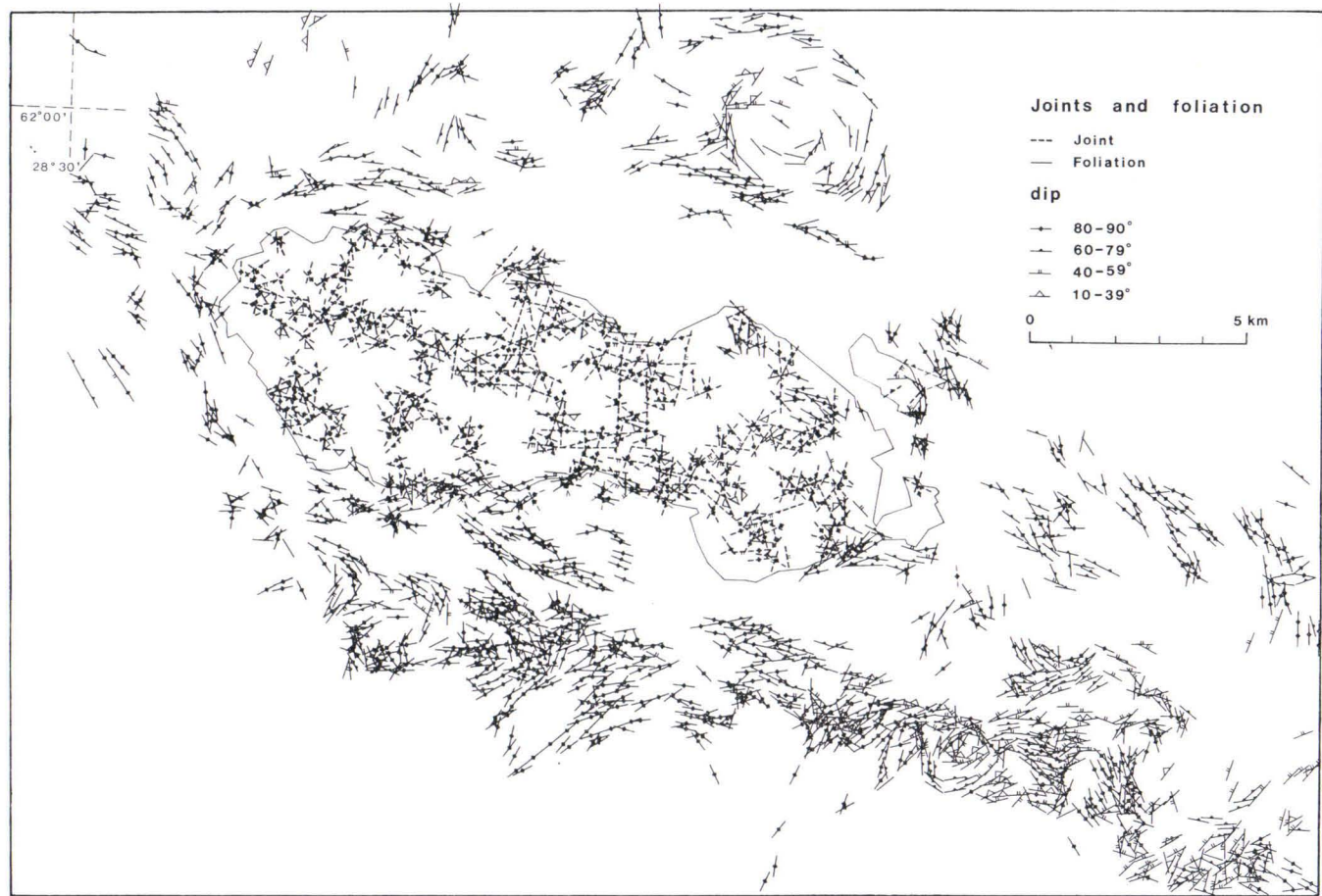


FIG. 17. Joints and foliation of the southern Haukivesi area.

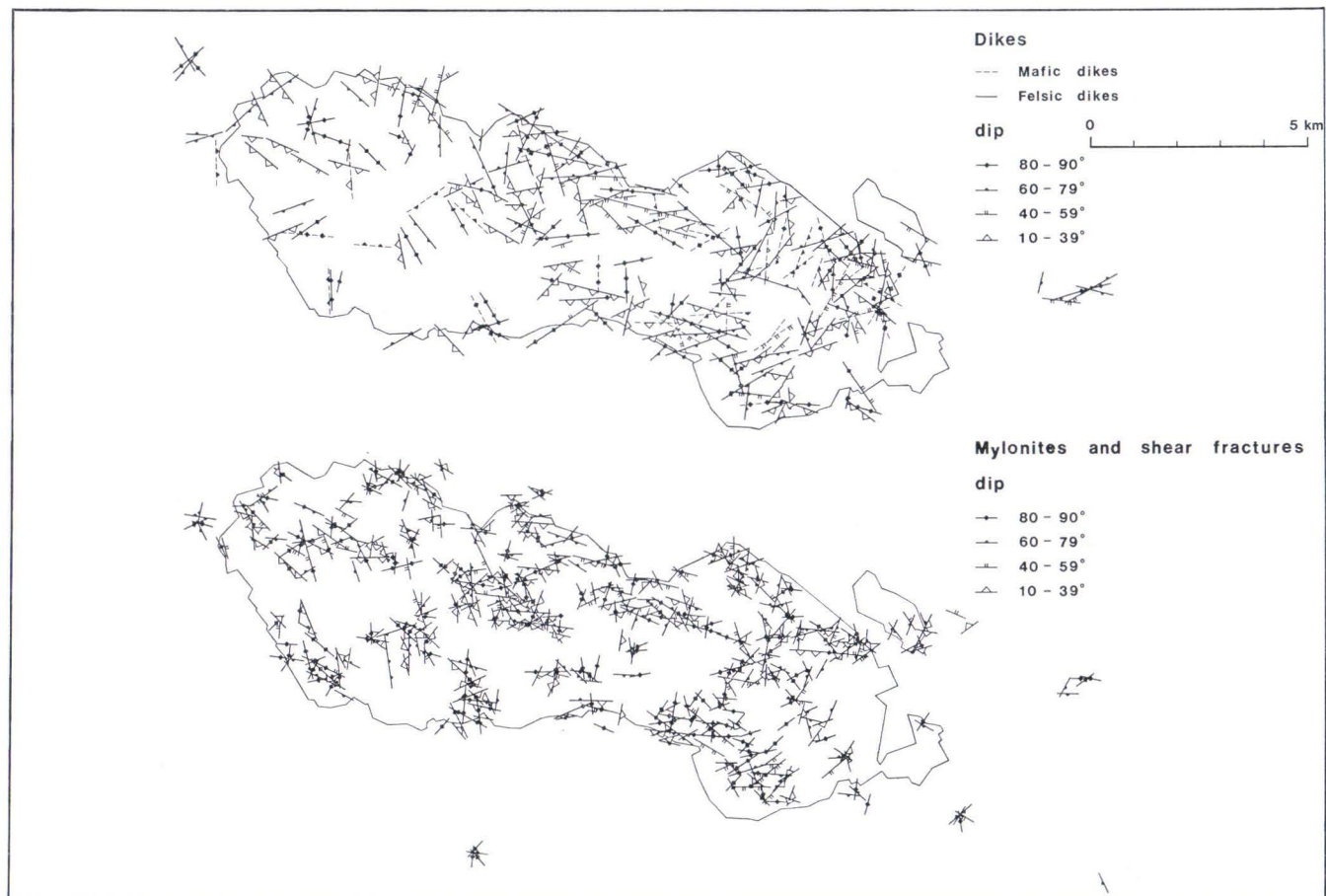


FIG. 18. Mafic and felsic dykes, mylonites and shear fractures of the Joutsenmäki mafic intrusive body.

of the fold axes on the one hand and the lineations on the other. Lineations plunging gently to  $270^\circ$ ,  $090^\circ$ ,  $305^\circ$ ,  $125^\circ$  conform with the strike directions of the majority of the supracrustal formations in the Haukivesi area. The age of the lineations plunging relatively steeply to  $020^\circ$ – $070^\circ$  is difficult to determine. It may be inferred from the rarity of gently plunging lineations and the dominance of steeply plunging ones that the latter were superposed on the former. The diversity of the plunge directions of the lineations as well as the bending and folding exhibited by the fold mullions of the amphibolites in the Savonlinna region and, especially, the bending of elongate conglomerate pebbles, are evidence for a polyphase folding of the supracrustal formations.

Several types and generations of foliation have been observed in the field (Fig. 36, diagrams 7–8). The oldest generation, bedding cleavage,  $S_1$ , has been destroyed by later generations. The dominant type, striking  $270^\circ$ – $310^\circ$  and dipping  $70^\circ$ – $90^\circ$  northeast, is schistosity,  $S_{2-3}$ . The youngest generation, with diverse strikes and steep dips, is crenulation cleavage,  $S_4$  (Figs. 13–14), which is encountered within shear zones. For all types of foliation the same symbol has been used in Fig. 17.

### Inside the intrusive

The lineations in the massif are mineral lineations of pyroxene and hornblende grains on the one hand and striations of slickensides on the other (Fig. 36, diagrams 2 and 4). They have different symbols on the lineation map (Fig. 16). Striations are rather rare and are probably connected with minor faults relatively young in age.

Two kinds of foliation have been observed in the intrusive. The older foliation may be a relic of magmatic flow structure (Figs. 3, 7 and 8).

The younger foliation (Fig. 8) has been observed in narrow shear zones, most frequently close to the contacts, especially to the northeast border of the intrusive. It is secondary cleavage with diverse attitudes and comparable with the crenulation cleavage in the surroundings of the intrusive (Fig. 37, diagrams 9–12). It is younger (Figs. 8–9) than the oldest mylonite and dyke generations of the intrusive.

The oldest fracture generation of the intrusive is that of the feldspar porphyric diorite dykes and breccias (Figs. 3, 5 and 8; Fig. 36, diagrams 1–2). It probably represents the deuteric fracturing and crystallization or recrystallization of the intrusive. The dykes are usually less than 1 m thick.

The most common felsic dyke rock is oligoclase pegmatite (Fig. 37, diagrams 7–12). In this study, pegmatites are treated together with the relatively rare fine- to medium-grained granite and trondhjemite dykes. Pegmatite dykes are generally less than 5 m thick, and most of them dip gently south to southwest (Fig. 18).

In the eastern part of the intrusive, mafic dykes, often from 5 to 10 m thick, are common (Fig. 18; Fig. 37, diagrams 3–6). In many cases they are composite dykes in which two to four components form thin and intensely folded bands or fold

mullions (Fig. 9). The composition of the bands varies from gabbro to quartzdiorite. The plunge of the fold axes and mullions is generally subvertical, which indicates subhorizontal strike slip movements in the dykes during or after their emplacement. On some occasions, dykes have been found in close association with minor faults (Fig. 8). The mafic and composite dykes are often brecciated and even foliated. The deformation may be syngenetic with the differentiation in the dykes. These phenomena and the emplacement of some of the mafic dykes cutting the felsic dykes are probably young events, although the emplacement of the bulk of the dykes may have preceded that of the felsic dykes. The strike of the mafic dykes is mainly perpendicular to that of the pegmatites, that is  $015^\circ$ , and the dip is mostly steeply east-southeast.

Mylonites (Fig. 18; Fig. 37, diagrams 13—17) are defined as dyke-like formations, from 0.5 to 500 cm thick (seldom thicker), filled with a product of extreme cataclastic or dislocation metamorphism (Figs. 10—11), often flint crush rock with occasional pseudotachylyte streaks. All the major rock types and also some of the felsic dykes of the intrusive have undergone cataclastic metamorphism in some places. Most of the mylonites are situated inside crush zones several meters broad, most of which dip gently south to southwest. Inside the mylonitic portions of these zones ductile microstructures such as laminated flow structures and folding (Fig. 11) have also been observed. These features seem to be associated with extreme cataclasis rather than with the ductile mylonitisation (see Bell and Etheridge, 1974).

Mylonites are generally believed to have formed in a plutonic environment (Kazansky, 1972) on fault surfaces, and especially on thrust fault surfaces. In some cases, the sense of the displacement may be inferred from the striations that coexist with mylonites. These interpretations only apply, however, to the youngest dislocations within old faults, since the mylonites are evidently older than the striations on their contact surfaces.

According to Johnson (1967) and Brown and Helmstaedt (1970), mylonites may be formed in compressional zones in the same way as cleavage in slates. Mylonites may also be compared genetically with schistosity in shear zones (Ramsay and Graham, 1970). According to Higgins (1971), the varieties with pseudotachylyte streaks may be called protoclastic mylonites — ultramylonites. Protoclastic mylonites represent the early fracturing of the crystallized massif when it was still hot enough to melt or vitrify under shearing stress.

Shear fractures (Fig. 18; Fig. 37, diagrams 18—22) are defined as mylonites or slickensides less than 0.5 cm thick. Their attitudes and habits are such that sometimes they overlap mylonites and sometimes joints (Figs. 6 and 10).

Joints (Fig. 17; Fig. 37, diagrams 23—27) are defined as fractures with no filling, no visible traces of movements along them and no cataclasis. Their strikes vary, but northeast strikes and steep dips are frequent as in the case of mafic dykes.

All the fracture types mentioned also seem to favour certain zones characterised by cataclastic textures, local metamorphism and relatively strong weathering. In the aerial photos, these zones are often recognized as lineaments.

Since the use of fracture patterns to establish models of intrusive tectonics, such as those constructed by Balk (1948), has been criticized (Berger and Pitcher, 1970), the fractures with the most diverse origin and age — joints and shear fractures — have been omitted from the genetic considerations discussed in a later chapter. They still play an important part in the description and analysis of geological structures.

### Lineament maps

Three classes of lineaments were differentiated on the basis of size. The class III lineaments (Fig. 21) were drawn from 1 : 10 000 photographic maps and the class II lineaments (Fig. 22) from 1 : 10 000 topographical maps, 1 : 20 000 outcrop maps and 1 : 60 000 stereo photographs. The class I lineaments (Fig. 23) were drawn from 1 : 100 000 aeromagnetic and aeroelectric maps, 1 : 100 000 to 1 : 400 000 lake maps, topographical and gravimetric maps and also maps of the Quaternary deposits of Finland. One of the photographs and the outcrop map are in Figs. 19 and 20, and the gravimetric map is in Fig. 32. A preliminary lineament map, based on the 1 : 100 000 aerogeophysical maps, is in Fig. 31.

Lineaments (as defined by Hobbs, 1911) of surficial origin were disregarded as far as possible. Resultant structures were omitted in favour of componental structures, when recognized, to avoid a premature interpretation of the elementary material. Straight rather than curved lines were adopted to describe lineaments (1) to avoid the fallacy of weathered linear structures with a curved outline, especially those with a gentle dip, (2) to procure pictures comparable with other tectonic maps in Figs. 17—18 and 24—25, (3) to avoid missing faint penetrative structures and (4) to prevent confusion between faults and their drag features. In general, the lineament tracing technique adopted was that of Lattman (1958) and Haman (1961, 1964). The tracing technique employed in the contour maps was in principle that used by Gay (1972), although coloured maps replace stereo maps.

With the exception of the borders of some of the map sheets, changes in the lineament pattern can be interpreted as reflections of corresponding changes in the bedrock structure. For this reason several more or less continuous changes in the class III lineament density along north and west parallel zones are to be noted. On the other hand, north or west parallel lineaments are rare. These features may be interpreted as traces of minor uplifts and depressions. Another noteworthy feature is the wavy appearance of some zones of subparallel or gently zigzagging class II and III lineaments striking northwest and northeast (Figs. 21, 23, 30 and 31).

The intrusive is surrounded by a topographical basin 2 to 3 km broad and poor in outcrops. Half of this basin is covered by water, half of it by soil (Figs. 19 and 20). The surficial deposits of the area are rather thin, generally less than 5 m, so that a fairly homogeneous network of lineaments could be constructed. However, in Fig. 21 the lake areas appear blank and the areas covered by soil are zones of low lineament density.

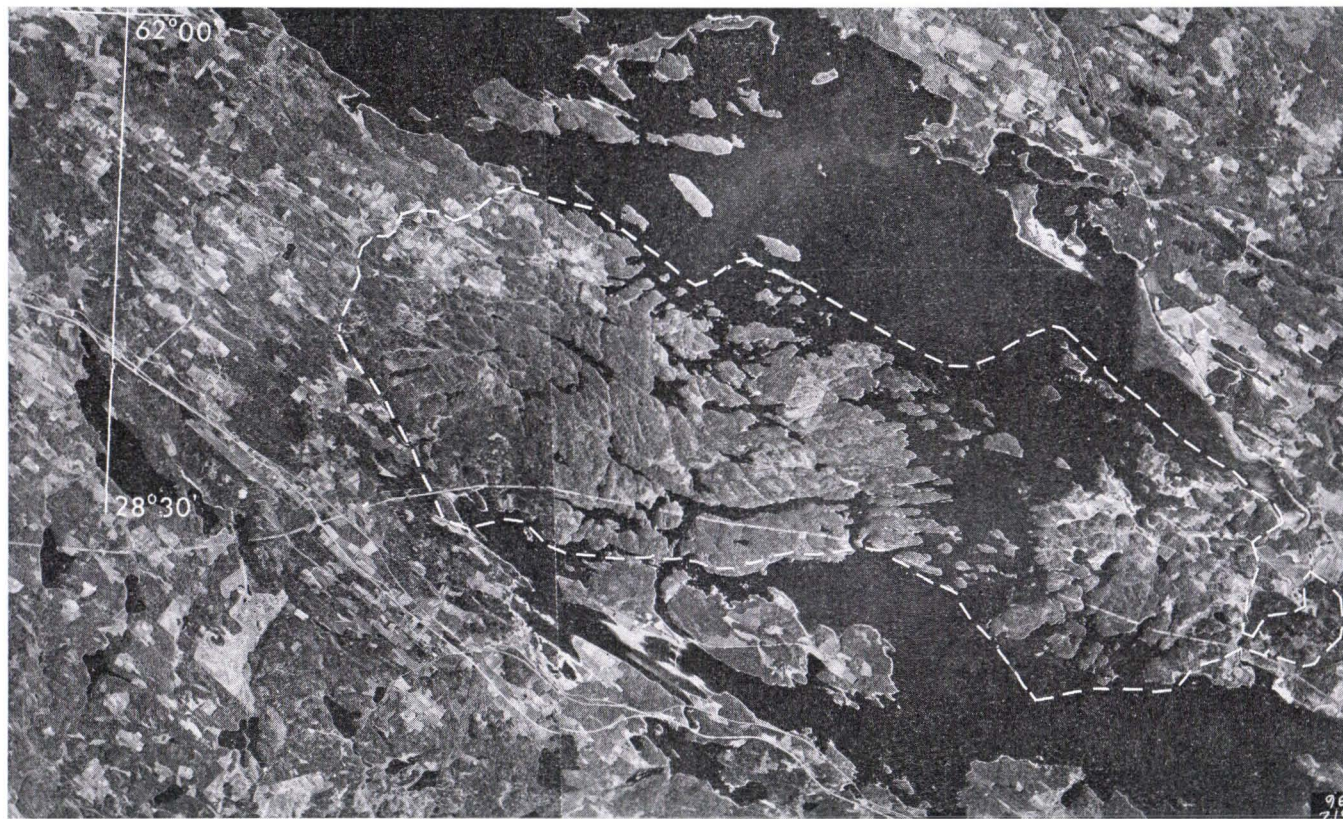


FIG. 19. Aerial photograph of the southern Haukivesi area. The border of the intrusive is drawn with a dashed line.

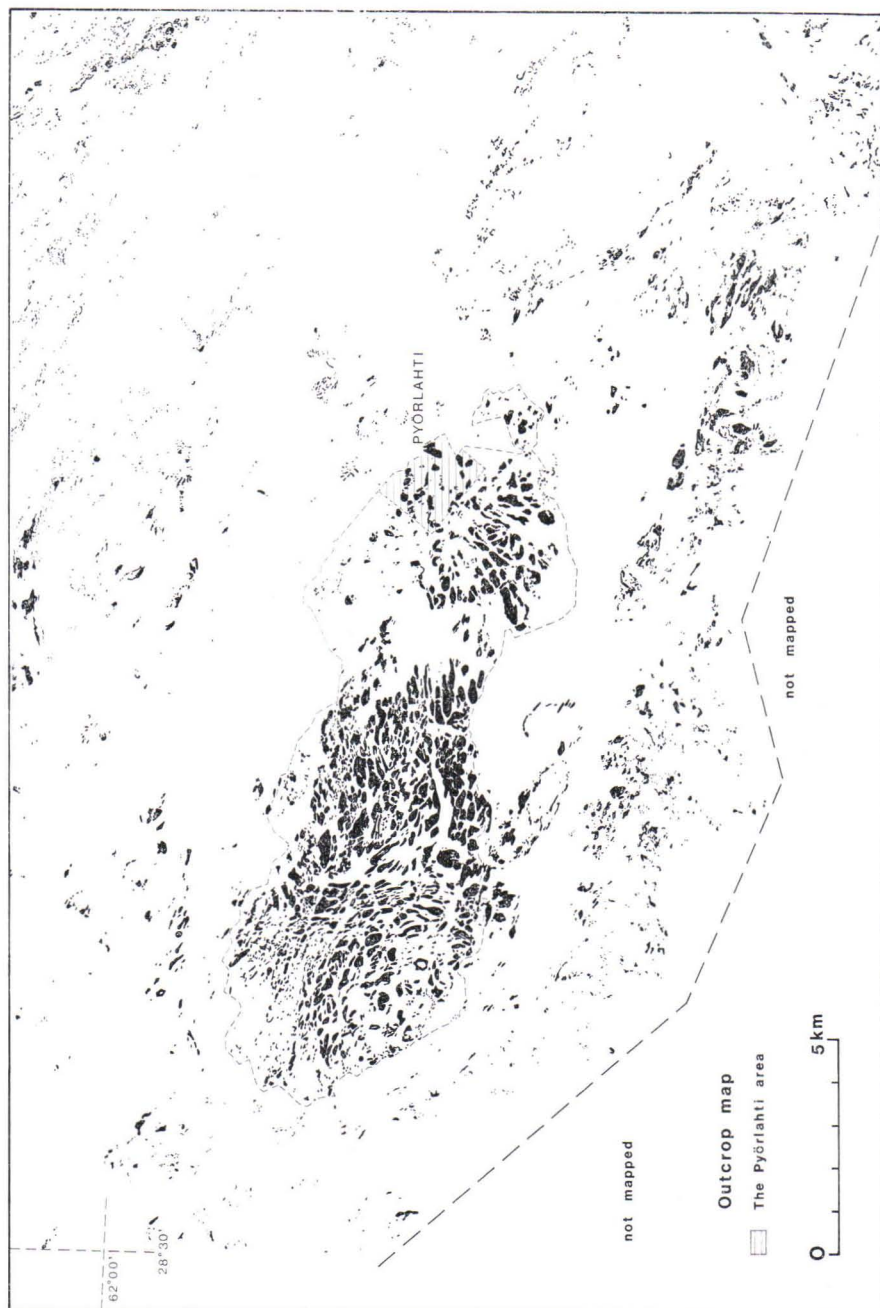


FIG. 20. Outcrop map of the southern Haukivesi area.



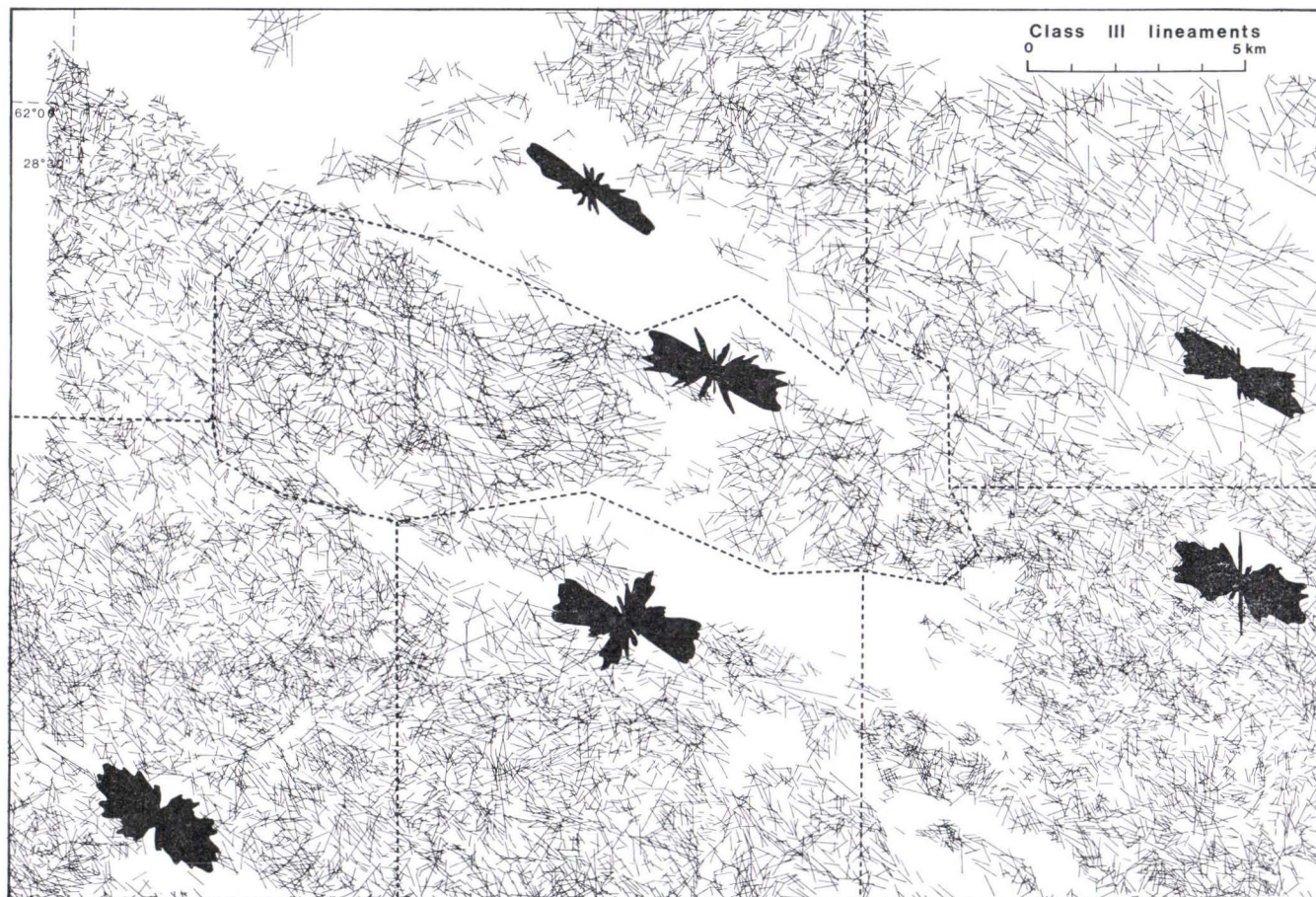


FIG. 21. Class III lineaments and the rosettes of class III lineaments of the southern Haukivesi area. The lineament frequencies were calculated by J. Aarnisalo, University of Helsinki, with a scanning optical filter (French FO-100, with automatic scanning facilities) using a 5°-sector filter.

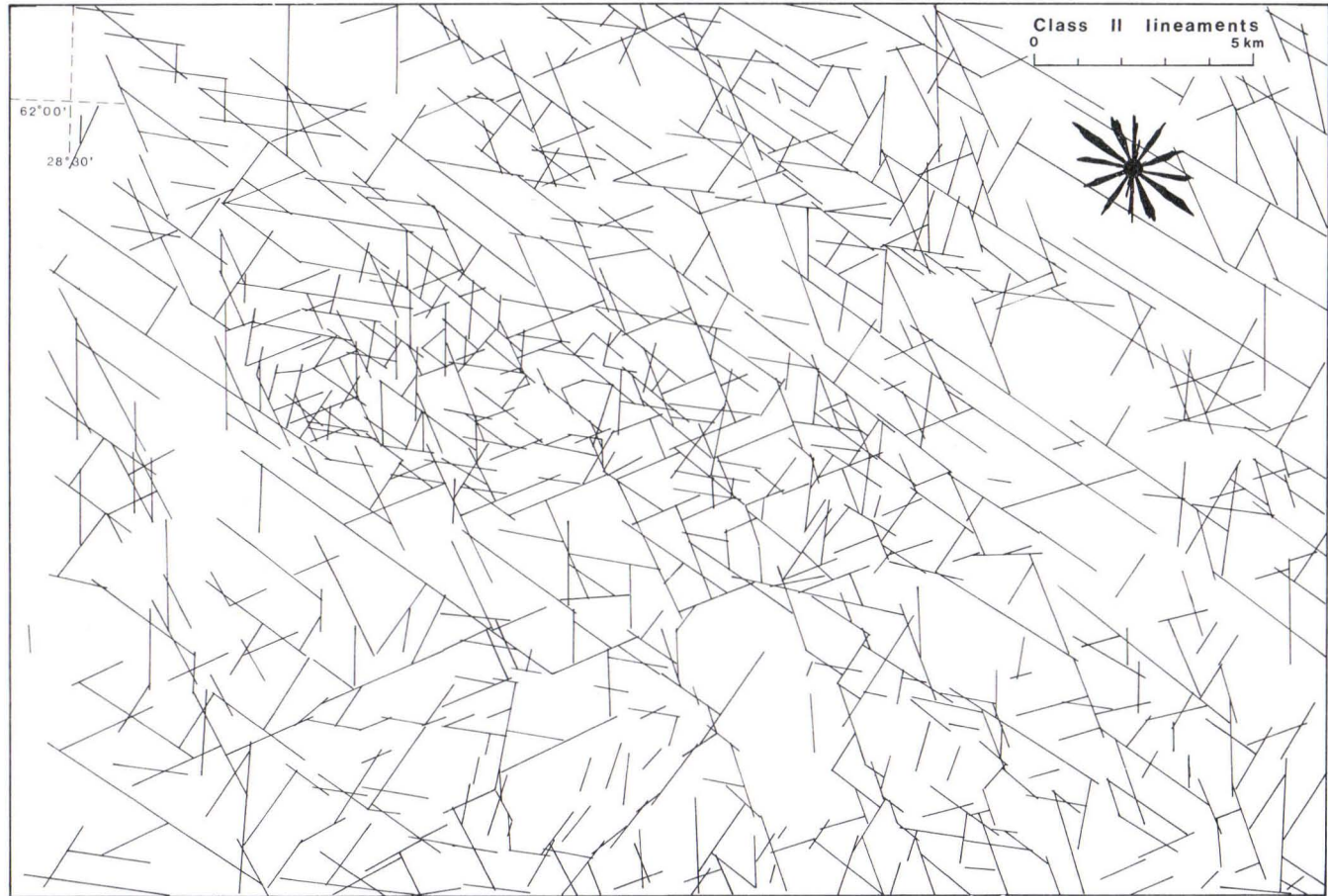


FIG. 22. Class II lineaments and the rosette of class II lineaments of the southern Haukivesi area.

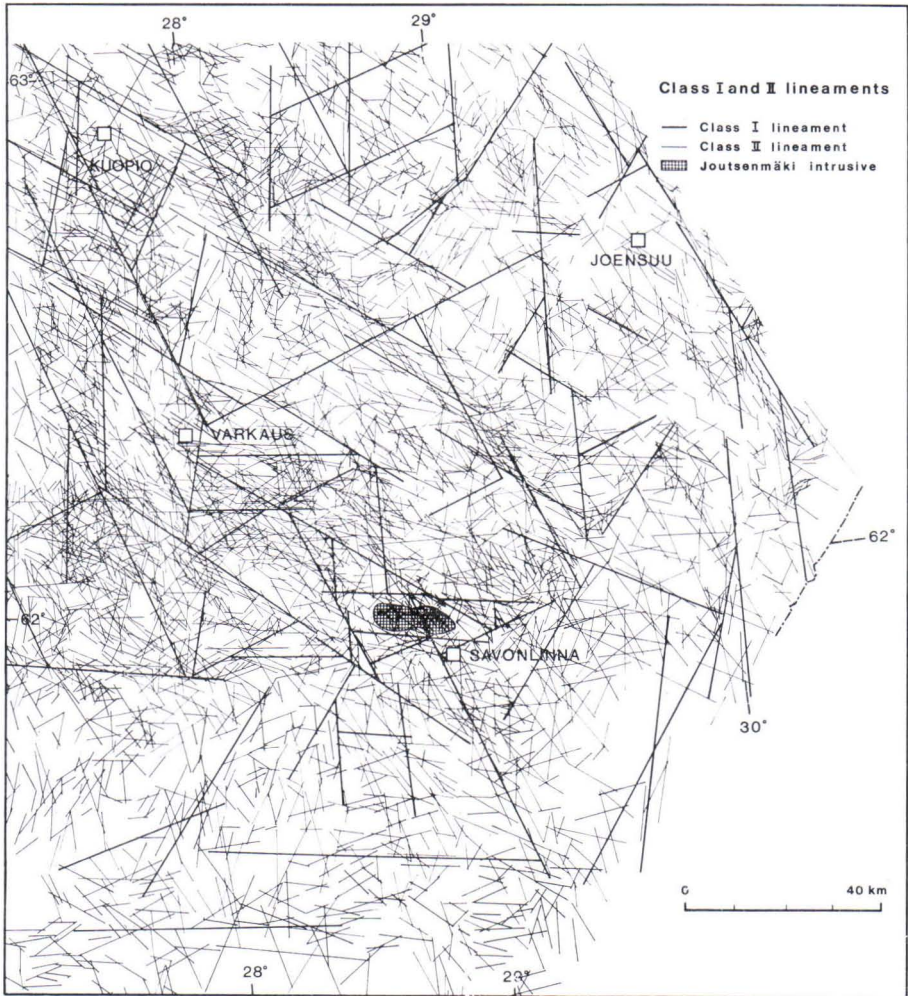


FIG. 23. Class I and II lineaments of the broader surroundings of the intrusive.

The map in Fig. 21 is divided into sub-areas, one of which constitutes the intrusive. The lineament strike frequency distribution (Tuominen *et al.*, 1973) of each sub-area is presented by a rosette.

Fig. 22 includes lake bottom topography. The lineaments appear in a much more coherent and regular pattern than in Fig. 21, one reason being that in the contour maps most structural details are omitted or smoothed. The result gives a picture of block-like fracturing in the investigation area. Some single movement zones are indicated by the continuity of lineaments especially in 280°, 305°, 335° and 070° directions. Of these only some 305° and 335° striking zones run indisputably through

both the intrusive and its surroundings, thereby indicating that they are zones of relatively young or long-lasting movements.

The strikes of the lineaments of classes I and II often coincide but in many areas and within many zones the class II lineaments are zigzagging or they form an echelon pattern around the class I lineaments. These features may indicate that the class I lineaments are rougher approximations of complex movement zones than the class II lineaments. Another explanation is that the lineaments of different classes mark structures of different orders that may have been formed simultaneously or successively. One further explanation may be that the classes of lineaments refer to different depths or depth dimensions of movement traces or faults.

The class II lineaments are analogical to the ones studied by Talvitie (1971), although he discarded those shorter than three kilometers to avoid traces caused by bedrock joints and other small features. The class I lineaments are roughly analogical to the lineament sets of Talvitie (1971). The difference is caused by the methods employed in the present study.

### Classification of foliation, fractures and lineaments

Foliation and fractures were classified according to their dips (Figs. 24 and 25). Fractures, shear zones and lineaments were classified according to their length and width (Table 1).

The lines in Fig. 24 refer to fractures and foliation with gentle dips (10—39°), and in Fig. 25 to fractures and foliation with steep dips (40—90°). Shear zones are drawn with heavy lines. They consist of dense swarms of subparallel shear and mylonite fractures or crenulation and secondary cleavage.

The dominant dip of the steeply dipping fractures and foliation is to the north, northeast and east. Inside the intrusive dips to the opposite direction are also visible. The gently dipping fractures in the intrusive dip mainly to the south, southwest and southeast, but foliation tends to dip to the opposite direction.

The dimensions of fractures (Table 1) are estimates based on field observations. The lengths of shear zones and lineaments have been measured from the respective maps (Figs. 21—23 and 25) the widths being estimates based on the interpreted map material.

TABLE 1

Lengths, widths and classes of fractures, shear zones and lineaments.

Fig.	Length km	Width m	Class
17, 18 .....	0.001—0.2	≤ 5	IV
21, 24, 25 .....	0.1— 2.0	5—200	III
22, 23, 25 .....	0.5— 20.0	10—500	II
23 .....	15.0— 80.0	500—2000	I

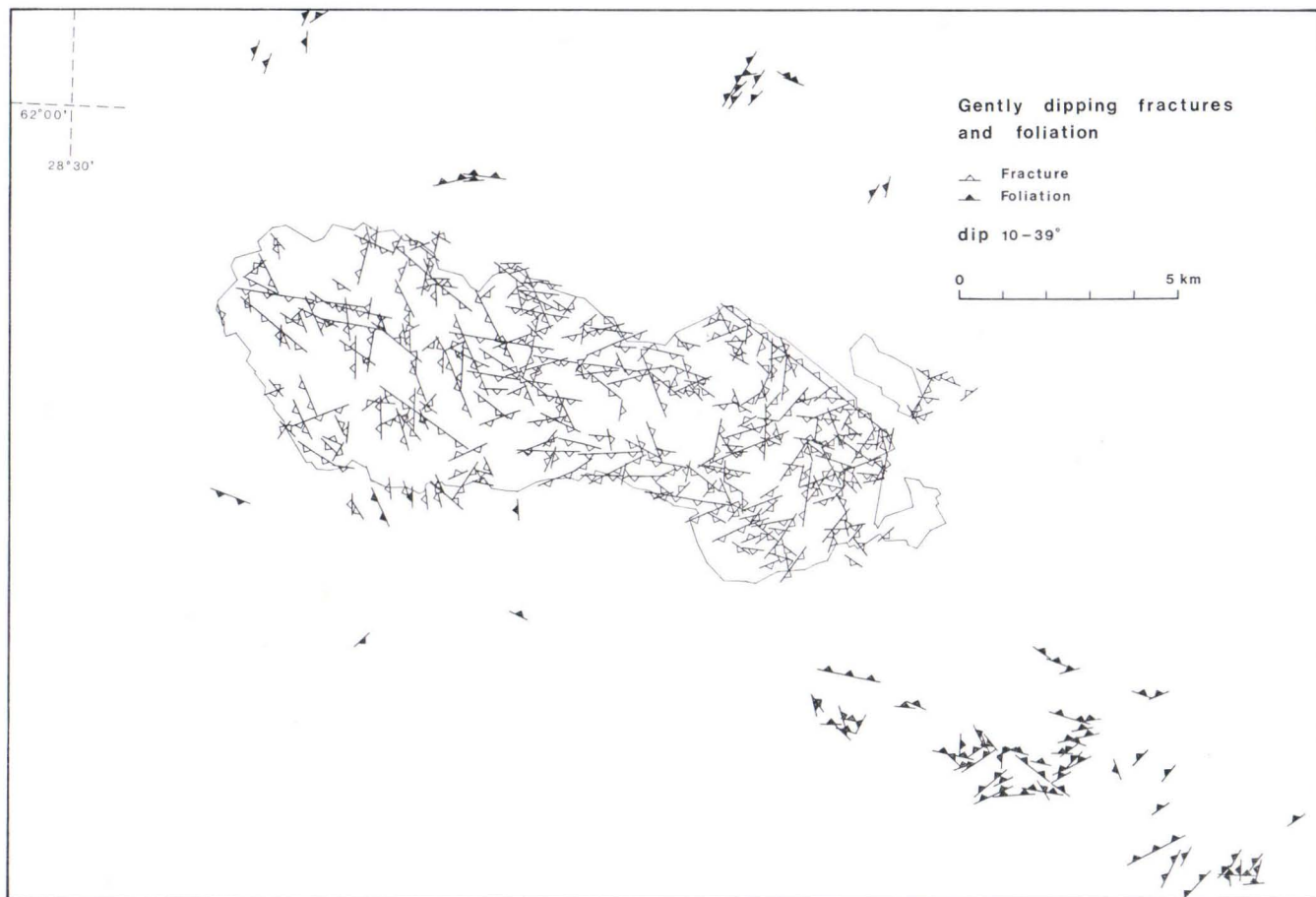


FIG. 24. Gently dipping fractures and foliation of the southern Haukivesi area. Generalized from the maps in Figs. 17 and 18.

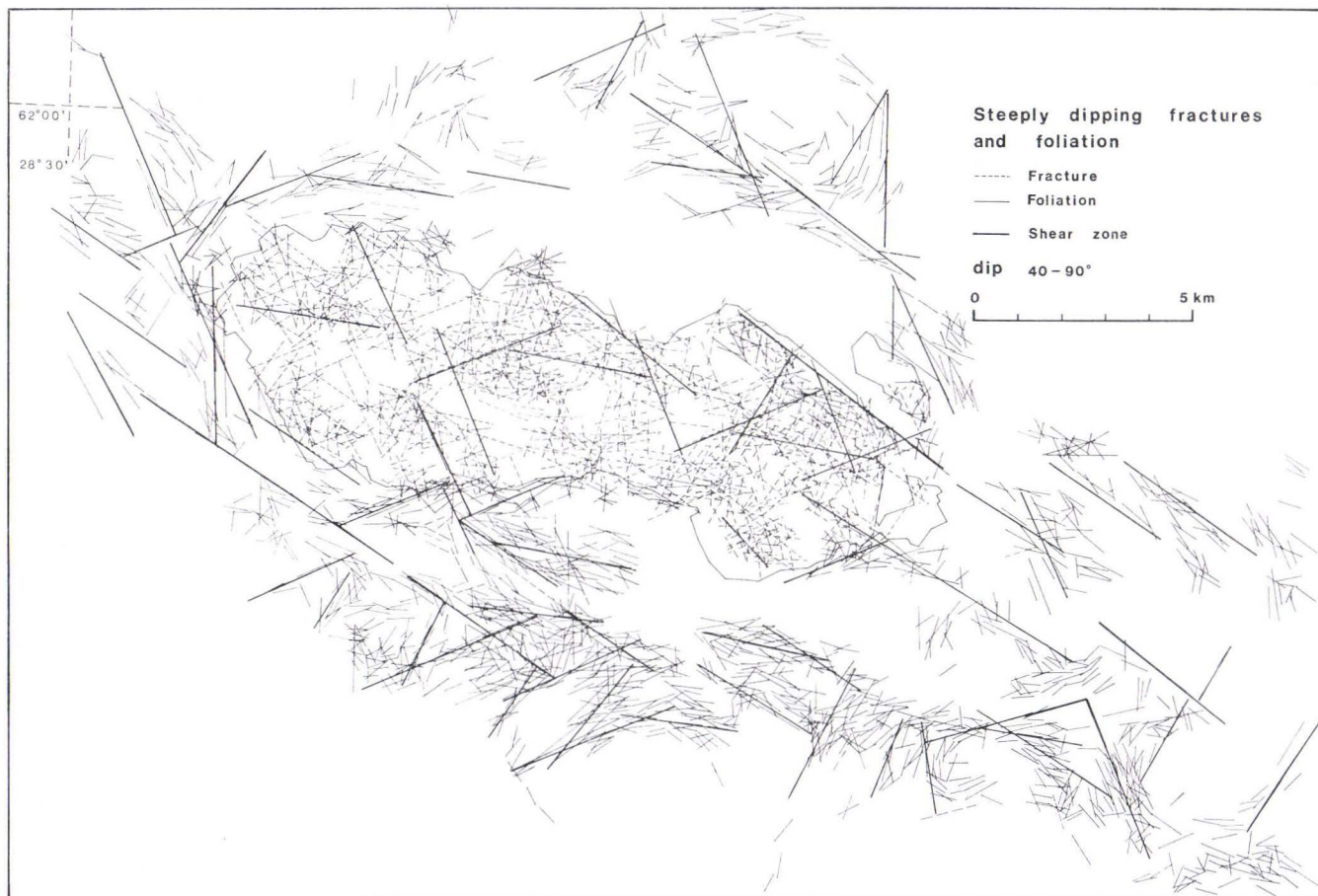


FIG. 25. Steeply dipping fractures, foliation and shear zones of the southern Haukivesi area. Generalized from the maps in Figs. 17 and 18.

The four size classes overlap each other, and the sources of interpretation are heterogeneous. Therefore, this classification is purely tentative and descriptive.

The generalized derivatives of the fractures of the intrusive can be compared in size with the class III lineaments. The shear zones of Fig. 25 are comparable with the class II lineaments of Fig. 22.

The smallest interspaces between subparallel class I, II and III lineaments tend to be 11 to 14 km, 1.2 to 1.8 km and 0.1 to 0.2 km, respectively.

### Structural interpretations

The main criteria for determining the nature of the movements responsible for the traces observed are listed below. Figs. 26—32 serve to demonstrate some of the phases of the procedure, and the results are summarized in Figs. 29 and 33.

(1) Field evidence, deductions based on the petrographical and structural markers, and deductions based on drag features as interpreted from the maps.

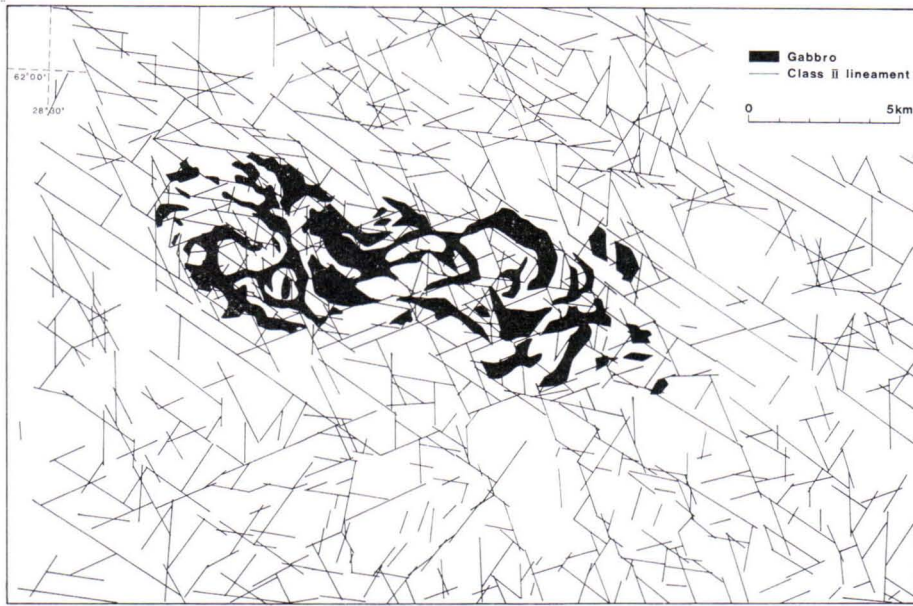
(2) Deductions based on the regional fracture and lineament geometry.

(3) Deductions based on the en echelon patterns exhibited by the component structural elements of complex tectonic zones. These include compressional features, such as foliation and mylonites, which form an angle of 0 to  $-45^\circ$  to the direction of movement. Shear fractures, the so-called »Riedel fractures», form an angle of 0 to  $+20^\circ$  to the direction of movement. There are also tensional fractures which form an angle of  $+45$  to  $+90^\circ$  to the direction of movement. These criteria have been discussed by Tchalenko (1970), Ramsay and Graham (1970), Gay (1972) and Wilcox *et al.* (1973).

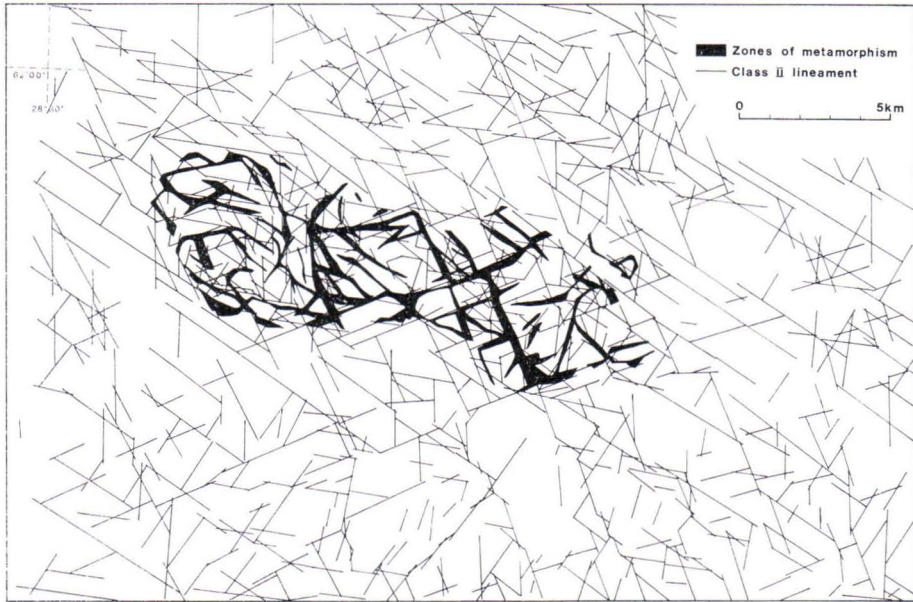
(4) Most of the criteria listed above apply to the recognition of transcurrent faults. The recognition of normal and reverse faults is more difficult and it has been based mainly on geophysical data. These include steep gravity slopes and ramps (Fig. 32), and border lines of areas in which the total intensity of the aeromagnetic field is considerably different from that of the surroundings. Yet the interpretations concerning normal and reverse faults are suggestions rather than conclusions.

### The intrusive

The six directional trends of class II lineaments in Fig. 22 apparently correlate with the petrographical characteristics of the intrusive. Many discontinuities in the gabbro zones seem to follow four main trends:  $305^\circ$ ,  $335^\circ$ ,  $035^\circ$  and  $070^\circ$ . Many of the discontinuities are also zones of metamorphism (Fig. 26). However, the structural and petrographical maps together give an impression of elliptical zoning in the middle portion and at the western end of the intrusive.



A



B

FIG. 26. Two maps of the intrusive with class II lineaments. A. The gabbro zones of the intrusive. B. The metamorphosed zones in the intrusive.



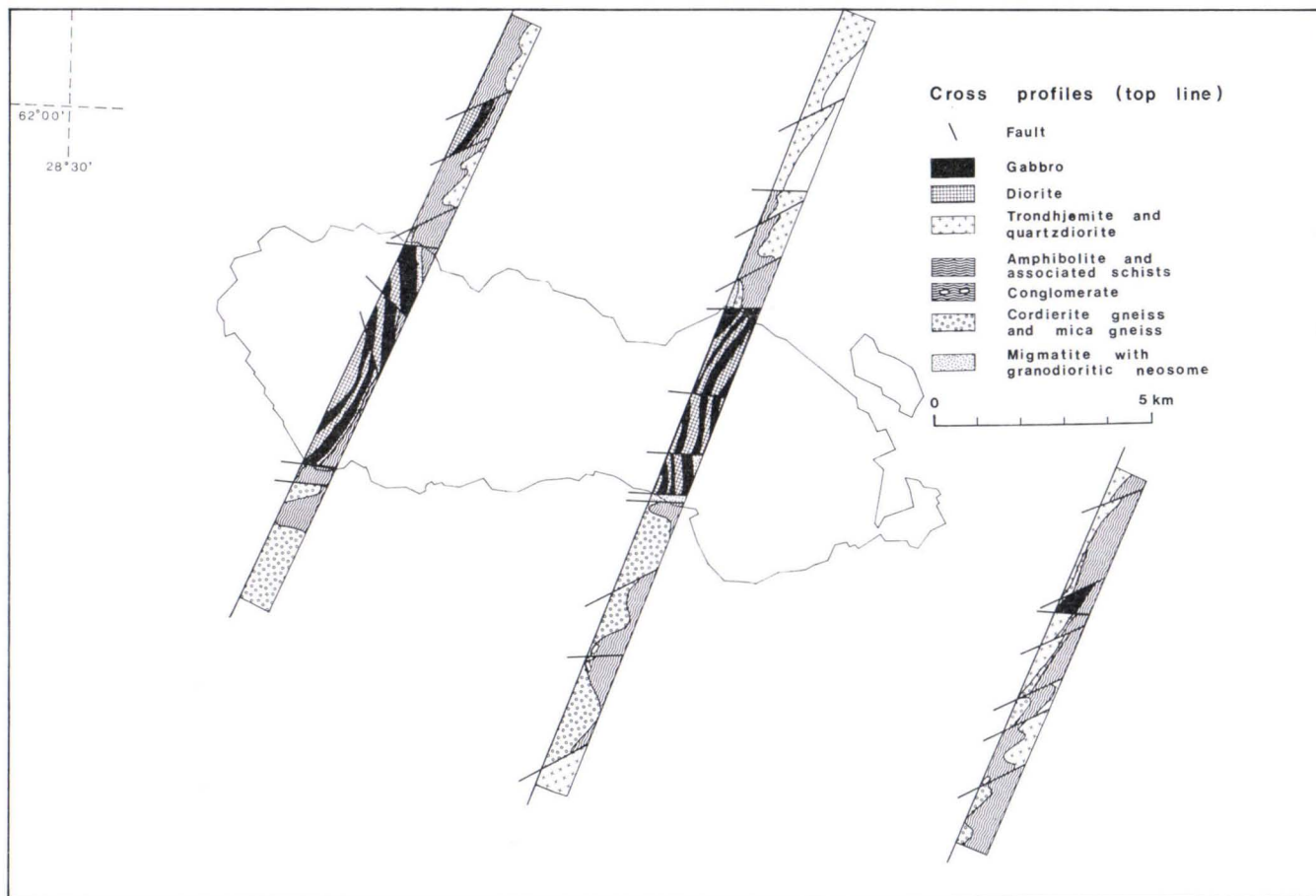


FIG. 27. Cross profiles of the southern Haukivesi area.

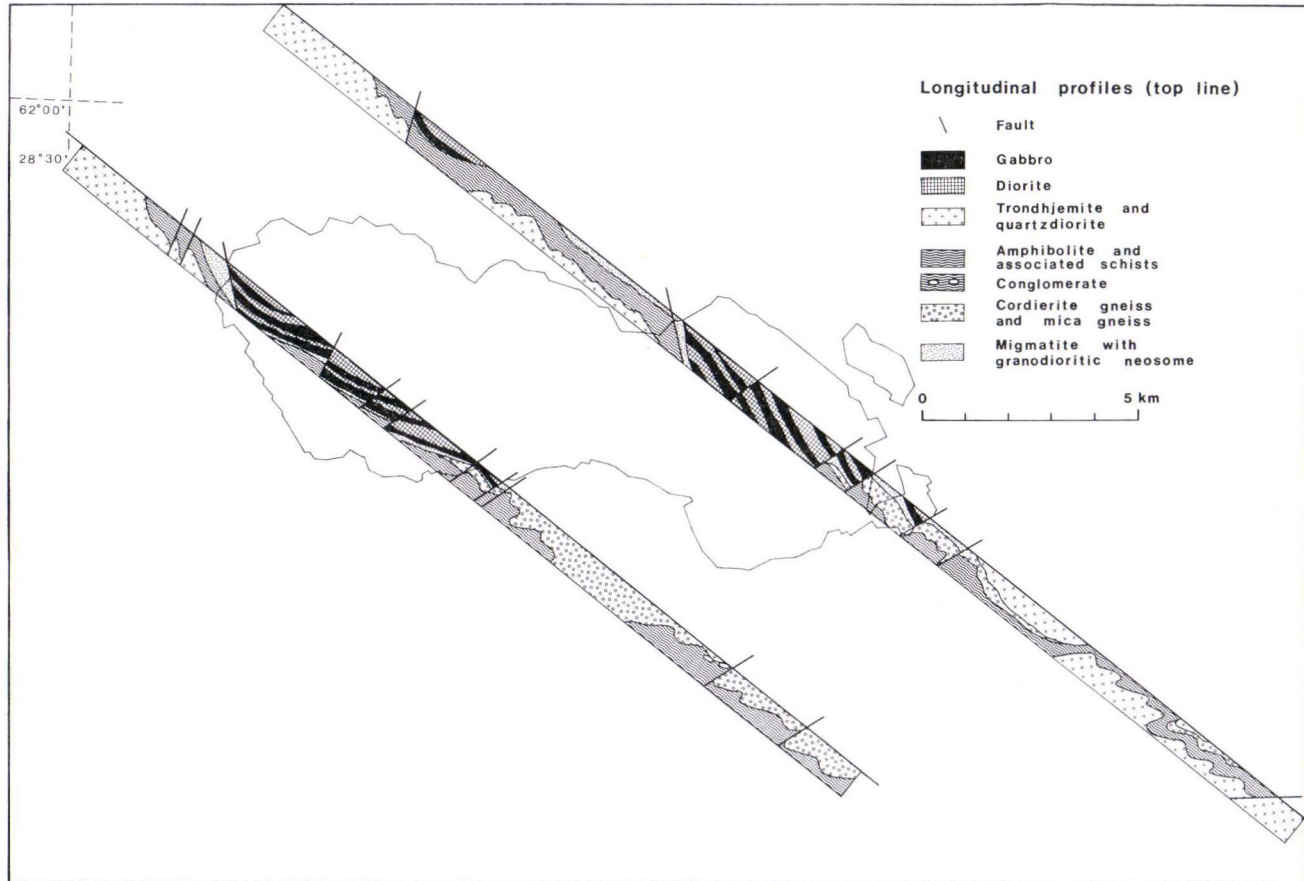


FIG. 28. Longitudinal profiles of the southern Haukivesi area.

Both the petrographical features and the patterns of gently dipping fractures and mineral lineations of the intrusive give an impression of a flat and relatively thin layered body. On the basis of this hypothesis, several profiles were constructed across the intrusive (Figs. 27 and 28). In these profiles the mafic body is shown to have been split into a coherent breccia by successive faulting. The faults are constructions based on main shear, lineament and discontinuity zones in the petrographical and structural maps. Gently dipping fractures are mostly excluded since their influence on the major structures seems to have been of minor importance.

### **The southern Haukivesi area**

Since the bulk of the mylonites of the intrusive and most of the foliation outside the intrusive dip to south or north, trend  $280^\circ$  can be interpreted as a result of compression and as such it is the strike of the thrust structures.

It would seem that trend  $335^\circ$  should be a right, and  $035^\circ$  a left lateral shear direction. However, the situation must be more complicated because these trends play only a minor role in the regional strike slip faulting (Figs. 29—33), the key role being played by trend  $305^\circ$  (right lateral) and  $070^\circ$  (left lateral). Moreover, trends  $305^\circ$  and  $335^\circ$  are predominant in the northwestern part of the area and in the western portion of the intrusive, whereas trends  $035^\circ$  and  $070^\circ$  dominate in the eastern portion and south of the intrusive (Figs. 21—22). Hence, the trends may be interpreted as cogenetic:  $305^\circ$  with  $335^\circ$ , and  $035^\circ$  with  $070^\circ$ .

The interpretations are summarized in Fig. 29. It seems that the crenulation cleavage connected with strike slip faulting is superposed on the older foliations, the oldest of which forms complex fold patterns in the areas of thrusting (south and southeast of the intrusive; see Gaál and Rauhamäki, 1971) and relatively simple tight synforms in the areas of normal faulting (northwest of the intrusive and at the southeast corner of the area).

### **The broader surroundings of the intrusive**

Talvitie (1971) concluded that the fracture pattern of the Kuopio region indicates that the  $305^\circ$ -direction acted as a wrench direction of the first order, and Gaál (1972) based the construction of the Kotalahti Nickel Belt on wrench fault tectonics controlled by faults in northwestern directions. Fig. 30 is an interpretation of the lineament map by Talvitie (1971) of the Kuopio region. Certain curved features in the original map have been interpreted as drag features indicating the sense of displacement along the respective transcurrent faults. A similar interpretation is applied to the lineament map by the present author of the broader surroundings of the intrusive (Fig. 31). It is based on aerogeophysical maps.

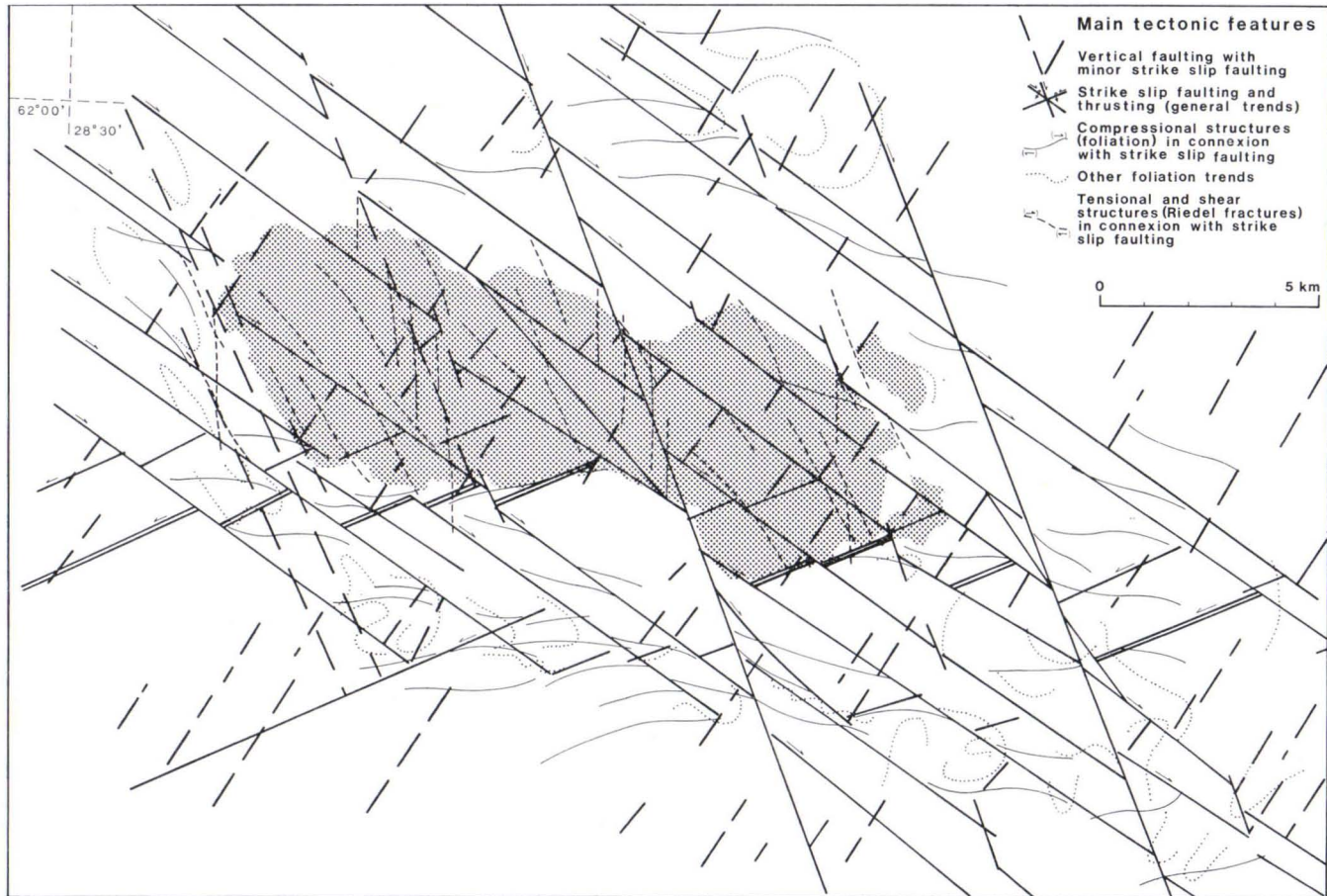


FIG. 29. Main tectonic features: faults with their associated tensional and compressional structures and foliation trends. A possible tectonic marker horizon, close to the southern border of the intrusive (shadowed) and split by younger transcurrent faults, is indicated with double lines.

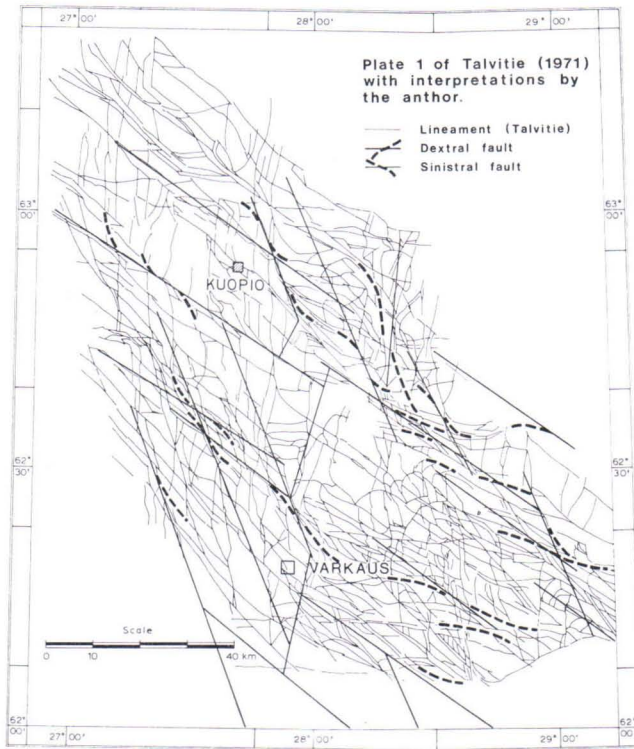


FIG. 30. Plate 1 of Talvitie (1971) with interpretations by the author: transcurrent faults and associated drag features.

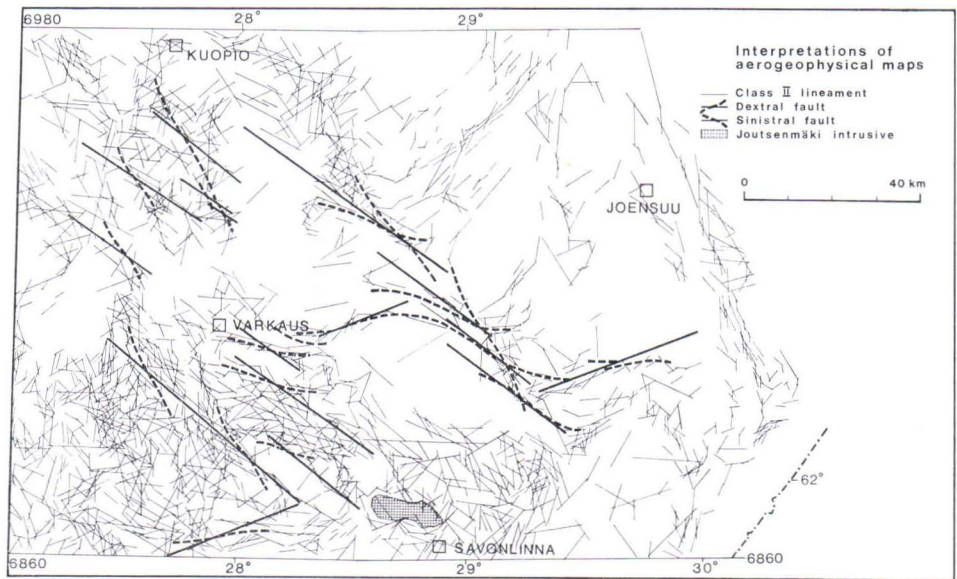


FIG. 31. Class II lineaments and transcurrent faults interpreted from the aerogeophysical maps.

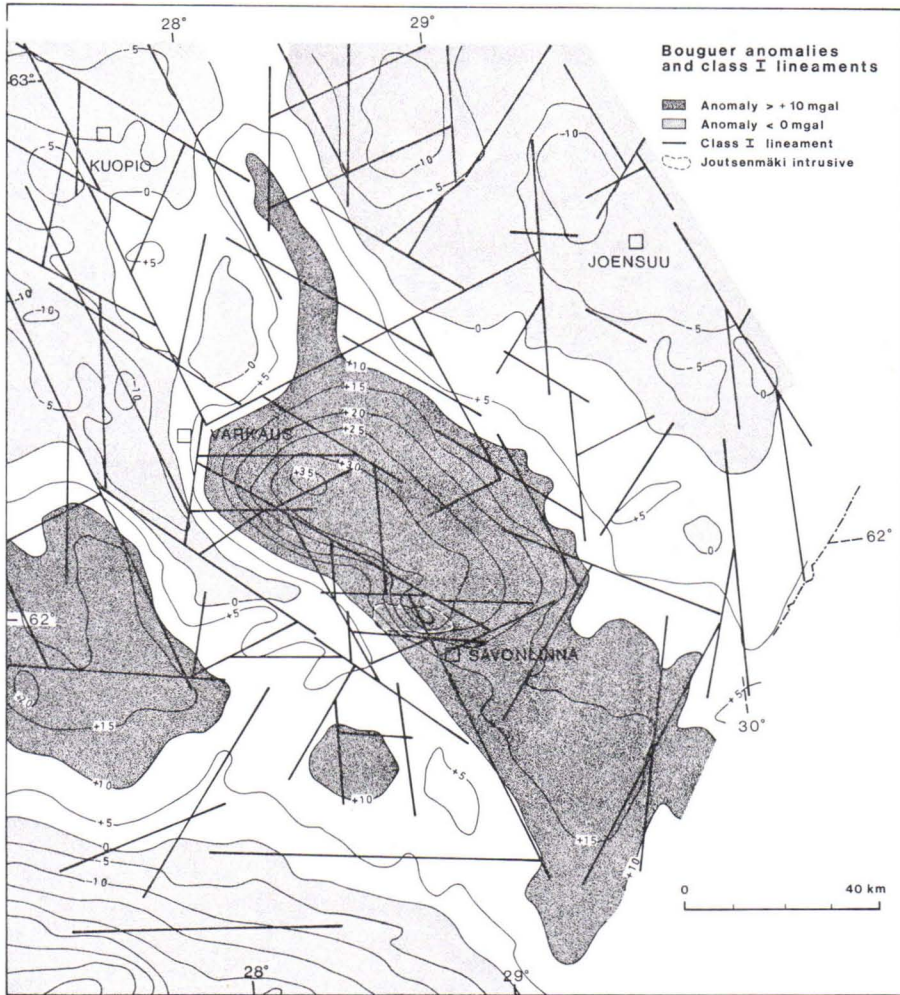


FIG. 32. The Bouguer anomaly map of eastern Finland by Honkasalo (1962) and the class I lineaments from Fig. 23.

In the interpretations two puzzling characteristics emerge. (1) In a certain area, roughly east of 28 degrees longitude, the 305° striking lineaments seem to be connected with right lateral faults. West of that longitude the 305° striking lineaments seem to be connected with left lateral faulting. Northeast from Savonlinna some 305° striking lineaments seem to be connected with both left and right lateral faulting. (2) Throughout the Haukivesi area, the left lateral trend dominates in large structures related to the 305° striking lineaments and the above variability is restricted to structures of the order of the class I lineaments. These features indicate that the 305° striking lineaments are traces of old and complex fault zones.

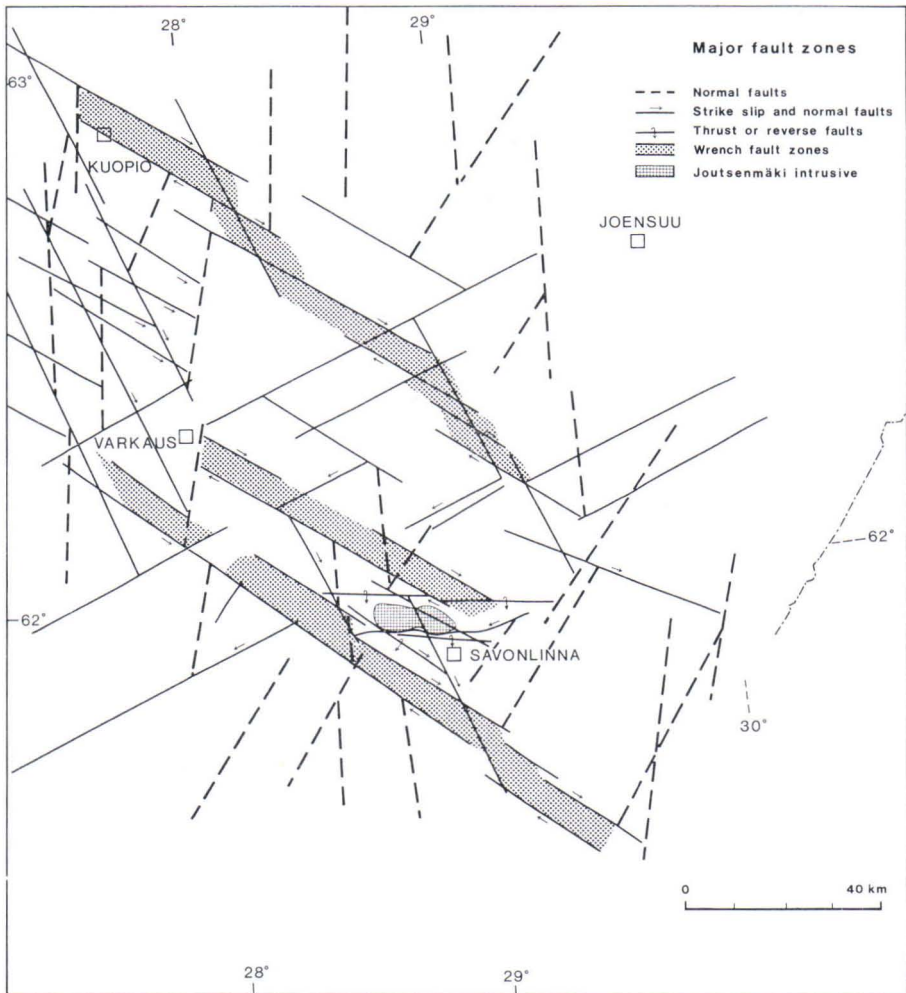


FIG. 33. Major fault zones and lineaments of the Haukivesi area and its surroundings.

Some of the consequences of these interpretations are shown in Fig. 33. They are probably most applicable to the youngest regional movements.

In Fig. 33 most of the faults are complex structures. It seems that most of the faults striking  $335^{\circ}$ ,  $000^{\circ}$ ,  $010^{\circ}$ – $015^{\circ}$  and  $035^{\circ}$  are primarily normal, and most of the faults striking  $305^{\circ}$  and  $070^{\circ}$  are both transcurrent and normal. The faults striking  $280^{\circ}$  may be thrust or reverse faults. However, the thrust faults in the Haukivesi area do not form single, linear zones, but rather the lines in Fig. 33 indicate a general trend of thrusting.

In Figs. 32 and 33 one further feature is emphasized. It seems that the great positive gravimetric anomaly (Honkasalo, 1962) north of the intrusive is surrounded

by 000° and 010—015° striking zones of faulting. The western succession of these fault zones seems to be the demarcation line between the forementioned right lateral (east of it) and left lateral (west of it) strike slip movements along faults striking 305°. These fault zones apparently mark the borders of the block whose internal structure is unlike that of the surroundings — at least that on the western side of the block. According to the fault map by Petrov (1970), there is no such demarcation line in the eastern border of this block.

### DATA TREATMENT

#### Correction of field data

In the field, mappers read the attitudes of structural elements to an accuracy of 1° (70 percent of the data) and 5° (30 percent of the data). Each reading was given in three digits starting right from 000° = north.

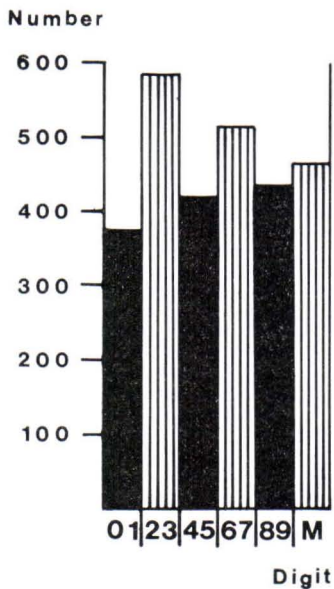


FIG. 34 The number of readings whose final digits are 0 or 1, 2 or 3, 4 or 5, 6 or 7, 8 or 9. M = the mean. 2330 fractures from the Pyörlahti area.

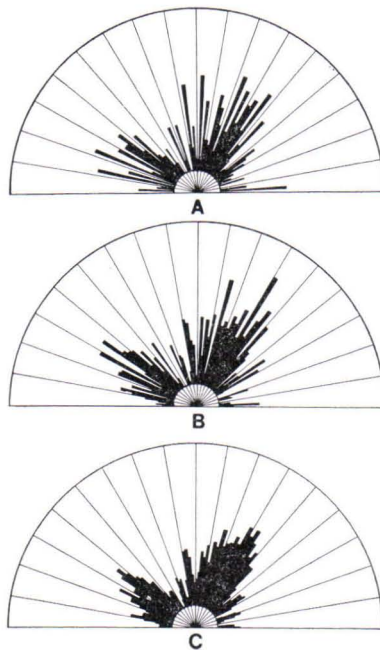


FIG. 35. The correction of the field data from the Pyörlahti area. 2330 fractures, dips 40—90°. A. Observed two-degree frequencies. B. Normalized two-degree frequencies. C. Smoothed two-degree frequencies.



Mappers tend to prefer certain digits to others. This number-preference (Söderholm, 1970) can only be recognized after the field measurements have been completed. The effect of number-preference is shown in Figs. 34 and 35. In many cases incorrect maxima are created at  $10^\circ$  intervals, true maxima being obscured or displaced.

To eliminate the preference for even or odd digits, the readings were first combined into successive two-degree groups:  $000-001^\circ$ ,  $002-003^\circ$ , . . .  $010-011^\circ$ , and so on (Fig. 35 A). The frequencies at the two-degree groups having the same last digits were then summarized. The sums are seen in Fig. 34. It is obvious that the differences between these sums result essentially from preferred final digits in the readings while the corresponding true frequencies must be nearly equal. For this reason the frequencies at each two-degree group were normalized by calculating their proportions of the respective sums (Fig. 35 B). The normalization of the frequencies may have caused certain errors which, however, do not seem to be significant.

The normalized two-degree frequencies were then smoothed by calculating the moving averages of three successive two-degree frequencies (Fig. 35 C). The correction method was also applied to the data read to an accuracy of  $5^\circ$ . The two groups of data were joined by summing up the normalized curves of strike-frequency distribution diagrams before the rose diagrams were drawn.

After the correction and summing up the diagrams were smoothed by a simple drawing procedure as shown in Fig. 36, diagram 18.

### Structural diagrams

The structural data of the southern Haukivesi area are presented on the equal area projection and rose diagrams in Figs. 36 and 37. The data are differentiated according to the qualities of the planar and linear elements. In addition, the planar elements are divided into two groups: attitudes measured from the whole of the intrusive and attitudes measured from the small Pyörlahti area inside the intrusive (as marked in Fig. 20). The latter are not included in the former.

For the rose diagrams the data were divided into two groups: planar elements with steep dips ( $40-90^\circ$ ) and those with gentle dips ( $10-39^\circ$ ). The orientations of linear elements with a steep and gentle plunge are so similar that differentiation according to the plunge is unnecessary. The distribution of structural elements according to their dips is shown in Table 2.

The strike-frequency distribution rosettes of the class III lineaments of the massif area and of the class II and III lineaments of the southern Haukivesi area are included in Fig. 36.

TABLE 2

Distribution of structural elements according to their dips (in percentages of the total amounts of elements). The amounts of horizontal and gently dipping fractures and foliation are minimum values because they are not easily recognizable. Therefore, the proportions of gently dipping felsic dikes (23.8 %) and mylonites (21.1 %) should be regarded highly significant.

Number and type of dip observations	10—39°	40—74°	75—90°	00—49°	50—79°	80—90°
4033 foliation .....	2.5	36.5	60.5			
980 lineation .....				37.7	55.1	7.2
156 lineation and striation ....				69.2	26.9	3.9
169 mafic dyke .....	10.6	50.3	39.1			
1601 felsic dyke .....	23.8	49.9	25.4			
1078 mylonite .....	21.1	55.1	23.7			
3908 shear fracture .....	17.0	42.3	39.3			
4854 joint .....	8.6	32.8	57.1			

### Regional trends of foliation, fractures and lineaments

The trends of the lineaments of the intrusive area and its surroundings show six azimuthal maxima, composed of mutually approximately perpendicular pairs (see Figs. 21—23, and 36). The same six maxima are visible in the foliation diagrams of the surroundings of the intrusive. These six maxima are 280°, 305°, 335°, 000°, 035° and 070° as measured at 28 degrees 30' longitude. Two less obvious maxima may be added, 290° and 010° or 015°. A summary of the correlations between the strike-frequency distributions of the structural elements and the above directional maxima is presented in Table 3.

Foliation, mylonites, felsic dykes and gently dipping fractures in general favour 280° to 305° strike directions. In the eastern half of the intrusive, the area represented by the domain of Pyörlahti, mylonites, mafic and felsic dykes also favour the direction 015—035°. The directional trend 290° is ambiguous because it is situated between two strong maxima. The explanation is the same as for the few other deviations from the above general pattern, that is, it reflects second order or small structures related to certain major ones.

### Strain and stress analysis

#### Theoretical considerations

$\delta_1$ ,  $\delta_2$  and  $\delta_3$  are the directions of the greatest, intermediate and least principal regional stresses. They can generally be considered as the directions of the minimum, intermediate and maximum total regional elongation, that is of axes  $Z < Y < X$  respectively, of principal finite strain.

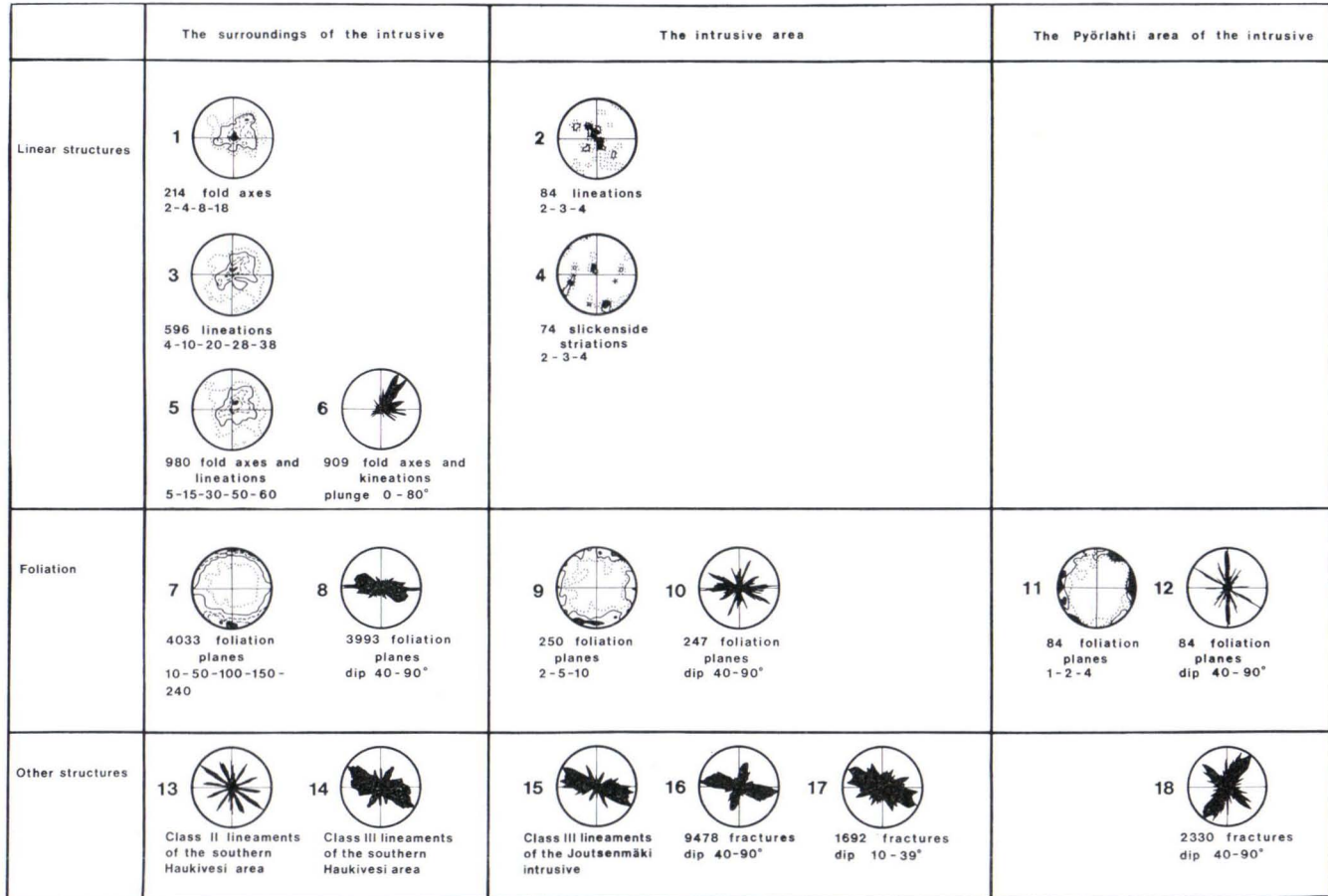


FIG. 36. Equal area and rose diagrams of the structural elements from the surroundings of the intrusive, the intrusive area and the Pyörlähti area of the intrusive.

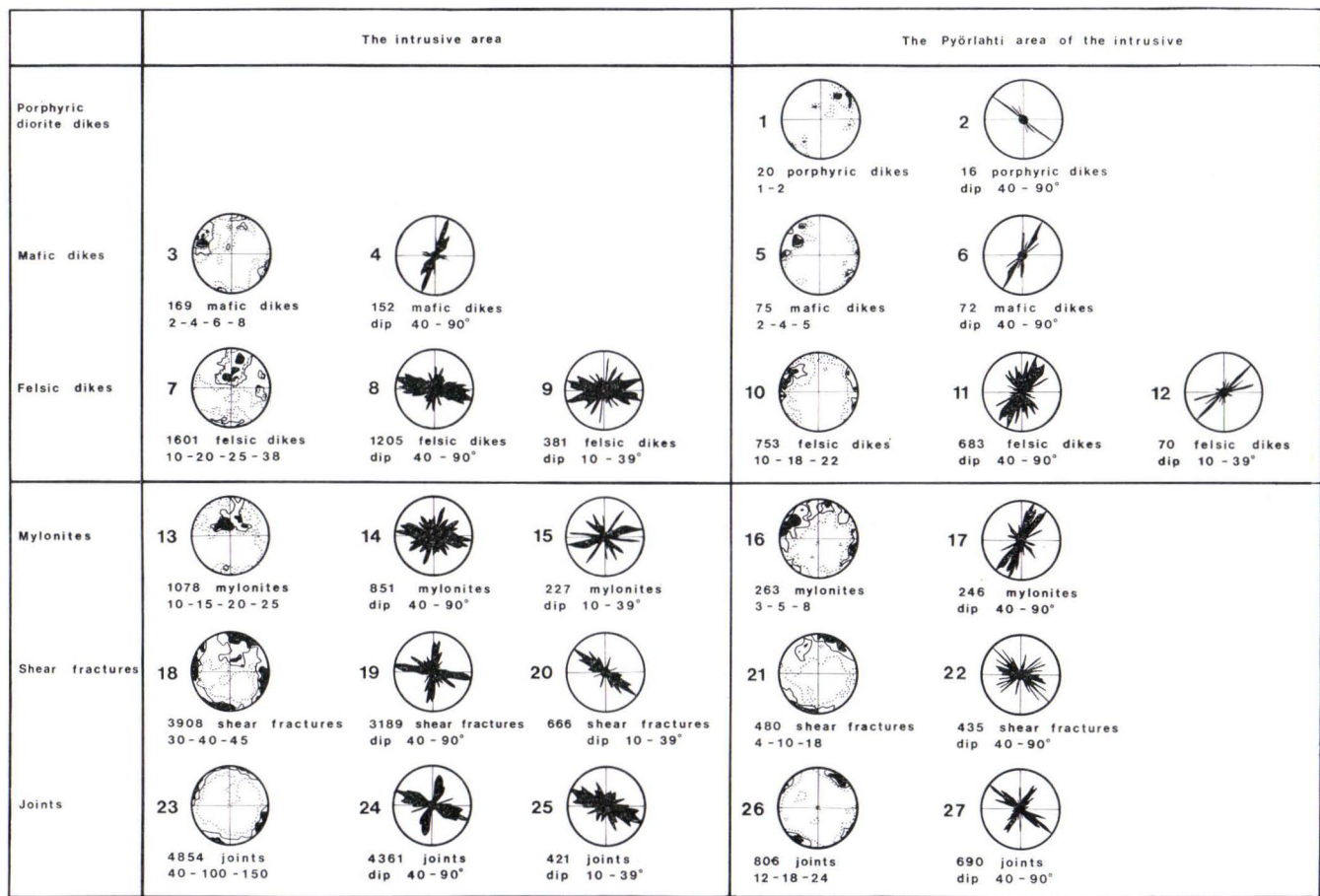


FIG. 37. Equal area and rose diagrams of the structural elements from the intrusive and the Pyörlähti area of the intrusive.

TABLE 3

The conformity of the strike-frequency distributions of various structural elements to the regional trends:

\*\*\* = the highest maximum in the strike-frequency distribution diagrams.

\*\* = a subsidiary maximum in the strike-frequency distribution diagrams.

\* = weak conformity.

— = no conformity.

Elements	280°	290°	305°	335°	000°	015°	035°	070°
Foliation .....	***	**	**	*	*	*	—	**
Lineation .....	*	—	*	—	*	***	***	**
Mylonites and shear fractures ....	***	**	**	*	*	**	**	**
Felsic dykes .....	***	***	*	**	*	**	**	**
Mafic dykes .....	*	—	—	—	*	***	**	—
Joints .....	**	***	*	*	—	**	*	*
Steeply dipping fractures .....	***	**	**	*	*	**	**	*
Gently dipping fractures .....	**	**	***	**	—	—	*	**
Class III (Fig. 21) lineaments ....	**	**	***	*	*	*	**	**
Class II (Fig. 22) lineaments ....	**	—	**	**	**	*	**	**
Class I (Fig. 23) lineaments .....	*	—	**	***	**	*	**	**

Foliation is generally thought to form perpendicular to  $\delta_1$  or Z (Wood, 1974) as a result of flattening. But conjugate crenulation or strain slip cleavage may form obliquely to the principal directions of strain (Means and Williams, 1972) and schistosity may also be transformed by simple shear parallel to it (Schwerdtner, 1973). In the present case, the interpretations will be based on the L-S tectonite fabric (Flinn, 1965) of which the planar element is parallel to the XY-plane of the finite strain ellipsoid.

Mineral and fabric lineations form in the direction of the major axis X (Ramsay, 1967; Schwerdtner, 1973), in certain thrust conditions parallel to the movement (Escher and Watterson, 1974) or, together with the fold axis, normal to Z in the en echelon folding of shear zones related to the basement wrenching (Wilcox *et al.*, 1973). In the L-S tectonites the linear element (fabric lineation) is parallel to the X-axis. Fold axes develop perpendicular to  $\delta_1$ , (Crosby and Link, 1972) or to Z, and they are either parallel or slightly inclined towards X or Y (Ramsay, 1967).

In an intrusive body mineral lineations may develop parallel to the direction of maximum flow (Ramsay, 1967; Dieterich, 1969; Pitcher and Berger, 1972) or by bodily rotational translation gliding normal to  $\delta_1$  (Nicolas *et al.* 1973).

Shear fractures and conjugate faults form at an angle of 20–45° to  $\delta_1$  and parallel to  $\delta_2$ . Extension or tensile fractures form parallel or slightly inclined to the  $\delta_1\delta_3$  plane. Normal shear fractures (Lajtai and Lajtai, 1974) form normal to  $\delta_1$ , that is, parallel to the  $\delta_2\delta_3$  plane. Longitudinal joints may develop parallel to the  $\delta_1\delta_2$  plane (Price, 1966; Mogi, 1973).

Second order and en echelon fractures associated with first order faults or shear zones will be discussed on the basis of contributions by Lajtai (1968), Price (1968), Tchalenko (1970) and Hancock (1972).

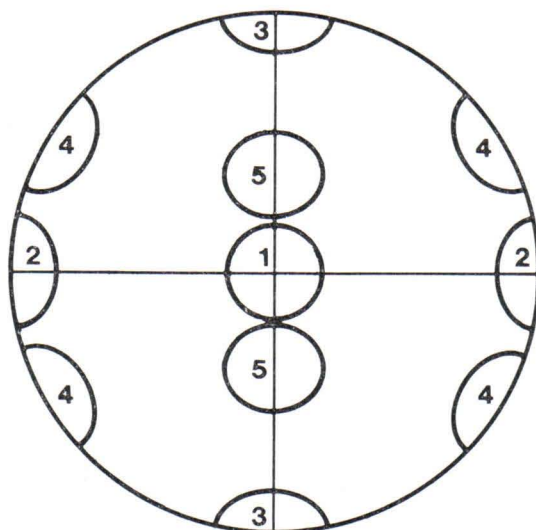


FIG. 38. A theoretical model for structures formed in a simple stress field with some variability in the relative strengths and in the directions of the principal stresses  $\delta_1$ ,  $\delta_2$ ,  $\delta_3$ . The orientations of  $\delta_1$ ,  $\delta_2$  and  $\delta_3$  are  $000^\circ$ ,  $270^\circ$  and vertical, respectively. The resulting foliation is shown by area no. 3, the fold axes by area no. 2, and the thrust faults by area no. 5. The conjugate shear fractures, transcurrent faults or strike slip faults possibly formed are shown by area no. 4. Area no. 1 represents the linear structures formed parallel to  $\delta_3$ .

The geometry of fractures and shears is a rather reliable means of determining the directions of the principal stresses even when the frictional properties of rocks and the  $\delta_2/\delta_1$  and  $\delta_3/\delta_1$  -relations vary (Jaeger and Rosengren, 1969).

During progressive deformation, the reorientation of pre-existing structures would result in the migration of the structural elements towards the positions determined by the existing strain (Escher and Watterson, 1974). For this reason, the construction of the deformation history of an area must start from the most recent processes. The exact determination of deformation paths has had to be omitted in this context with the exception of certain simple visually catchable structural features as shown in Figs. 2 and 16—33.

A theoretical model for structures created in a simple stress field with some variability in the relative strengths of the principal stresses is presented in an equal area diagram in Fig. 38.

### Practical consequences

The stress field models explaining the development of the structures of the southern Haukivesi area are grouped in Fig. 39. The orientations of  $\delta_1$  in groups I, II and III are  $035^\circ$ ,  $340^\circ$  and  $000-010^\circ$  respectively.

In Fig. 39 three variations of the group I stress fields are described; the principal stresses show shifting relative strengths and the plunges of the stress directions vary from subhorizontal or subvertical to inclined. The three variations of the group II stress fields are described in the same manner. Tensional, compressional and shear structures are indicated in the diagrams insofar as they have been encountered in reality.

In the light of kinematic considerations (see Figs. 29 and 33), the stress field models can be connected with each other so that two primary fields are left (I A, B and II A, B), the remainder being explained as secondary fields formed within wrench (III A, B) and thrust (I C, II C, III C) zones. Stress field IV alone seems somewhat rootless, and can be treated as a secondary field to I or as an independent field.

The  $\delta_1$  stresses of the primary stress fields are oriented  $340^\circ$  and  $035^\circ$  (Fig. 39). These are the most probable directions of tensional structures in general, steeply dipping fractures and dykes, as well as normal faults with related folding. The corresponding compressional zones should lie perpendicular to them and close to the planes  $\delta_2\delta_3$ . They are most probably defined by axial plane cleavage, fold axes and lineations, and reverse or thrust faulting with related folding and fracturing. The third primary group is formed by planar shear structures at an angle of  $35^\circ$  to  $\delta_1$  and parallel to  $\delta_2$ . The most prominent shear directions of the area are dextral  $305^\circ$  and sinistral  $070^\circ$ .

Regionally, the most prominent secondary structures are formed within wrenches (Wilcox *et al.*, 1973) in the primary shear directions and thrusts to the south-southwest and south-southeast. The secondary stress fields of the main wrenches have almost identical axial orientations. This hypothesis can be employed to explain the prominent east to west trends exhibited by the fracturing of the intrusive and the foliation in its surroundings.

The chief results of the secondary stress fields are thrusts (faults and folding) to the south-southwest and south, and tensional structures perpendicular to them. Some of the transcurrent faulting and wrenching, viz. dextral ( $335^\circ$ ) and sinistral ( $020-045^\circ$ ), can be explained as by-products of the former structures.

All the regionally conspicuous tensional, compressional and shear trends as exhibited by planar structures form a rather symmetric pattern, which is shown in Fig. 39.

## GEOLOGICAL POSITION AND DEVELOPMENT OF THE INTRUSIVE

### The location of the intrusive

The structural geology of eastern Finland, insofar as it is relevant to the present study, has been discussed by Härme (1961), Mikkola and Niini (1968), Talvitie (1971), Gaál and Rauhamäki (1971), Gaál (1972), Mikkola and Vuorela (1973), Tuominen

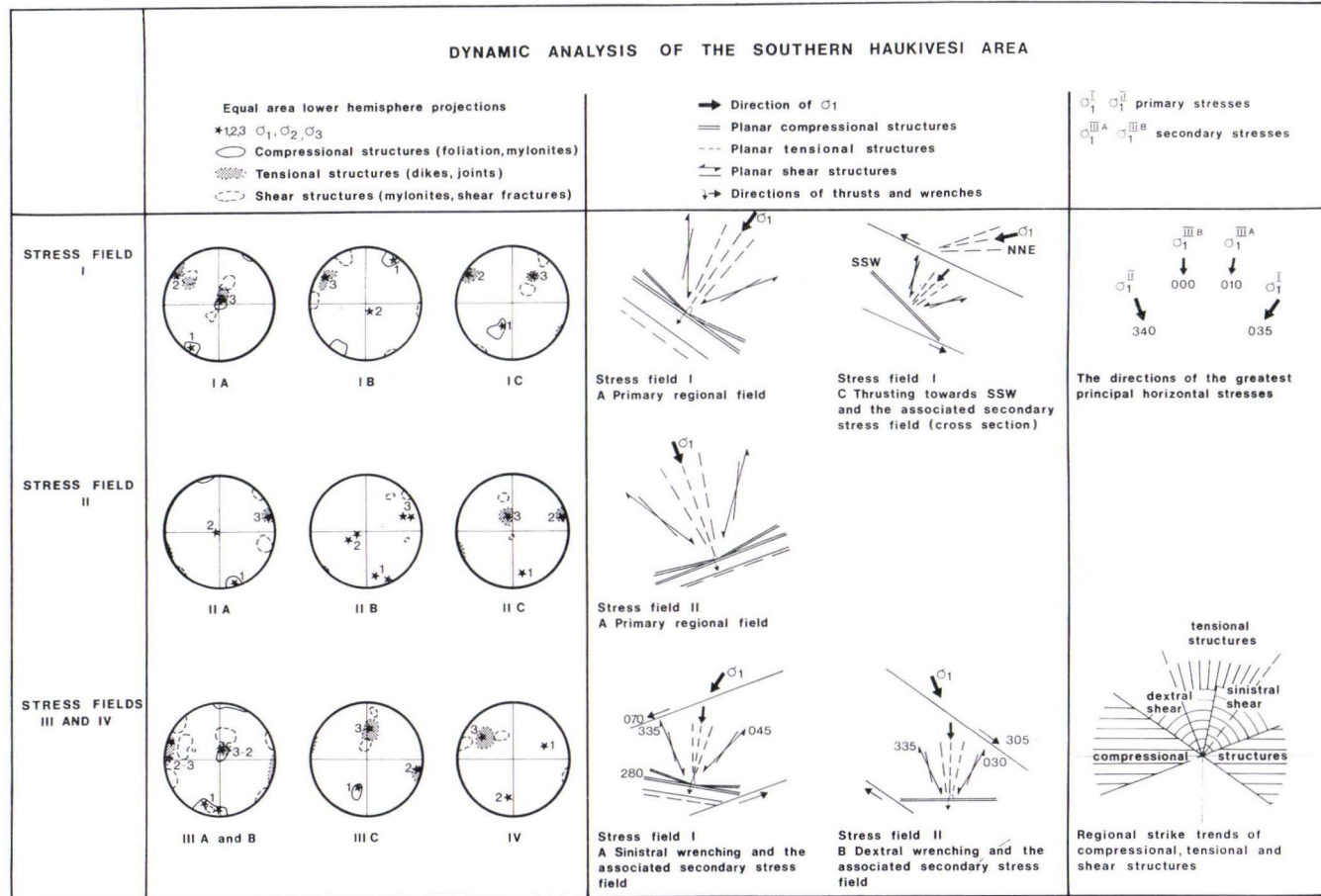


FIG. 39. Summary of the dynamic analysis of the southern Haukivesi area.



*et al.* (1973). The faults, fractures and lineaments interpreted by these authors do not fit in all details with those presented in this paper. The discrepancies are largely due to the diversity of areas, working scales, materials and methods employed. In these respects, the works by Gaál and Tuominen's team come closest to the present one.

However, there is no discord as to the general trends and certain details. The statistical strike-frequency distributions of foliation, Bouguer gravity isolines and fracture lines of Finland (Tuominen *et al.*, 1973) are consistent with the strike-frequency distributions of the lineaments and structural elements of the southern Haukivesi area. In most of the publications mentioned, the southern Haukivesi area is shown to be located at a junction of several major lineaments with dissimilar strikes.

The intrusive is located between two major dextral wrench zones with a strike  $305^\circ$  (Fig. 33). These zones are crossed by minor zones of dextral strike slip and normal faults with a strike  $335^\circ$ . The continuation of the northern wrench fault zone is not shown, but the supposed deformed features of an older, sinistral strike slip fault with a strike  $070^\circ$  (Fig. 29) indicate that it may run through the northeastern part of the intrusive. A set of thrust zones with a strike  $280^\circ$  and a dip to the north is presumed to be genetically related to the wrench faults. In addition, zones of major normal faults with strikes  $335^\circ$ ,  $000^\circ$  and  $035^\circ$  are characteristic of the area in Fig. 33.

These directional trends appear as directional maxima for different types and generations of structural elements although some regional variations are also present. Tectonic analyses indicate that the mafic body has undergone severe deformation since emplacement. In spite of the deformation some structural features have remained, such as the tabular, sill-like shape of the body and certain internal structural characteristics.

The intrusive seems to be situated in a shallow basin formed at the junction of synforms striking north-northwest and northeast (see Fig. 16; Gaál and Rauhamäki, 1971, Figs. 45 A, 54). The intrusive is underlain by rocks of sedimentary and volcano-sedimentary origin. The intrusive cuts the sedimentary sequence and is at its northern end in contact with the volcano-sedimentary amphibolites that belong to the lowest known stratigraphical horizon (Gaál and Rauhamäki, 1971). In the following the deformation phases of the intrusive will be treated starting from the most recent one, the post-intrusion phase II (Table 4).

### The post-intrusion phase II

The post-intrusion phase II covers a period subsequent to the final magmatic crystallization of the intrusive and, approximately, the period subsequent to the regional metamorphism of the southern Haukivesi rocks. The geological processes of this phase were restricted to local phenomena, such as the deformation and metamorphism of rocks within shear zones and the formation and deformation of felsic dykes.

The different generations of the structural elements, genetically significant, inside and outside the intrusive are grouped in Table 4 according to their relative ages and modes of origin as discussed earlier. The ages of the structural elements outside the intrusive are tentatively related to the phases of the intrusive.

The youngest mylonite generations and minor faults with associated striations can be attributed to this phase. The same applies to secondary cleavage (in the intrusive) and crenulation cleavage (outside the intrusive) in shear zones. The age of the composite dykes in the intrusive is somewhat problematic. Because of the rate of recrystallisation and plastic deformation during the formation of the dykes, they probably originated prior to this phase. It is likely that certain non-deformed felsic dykes as well as most of the joints in the intrusive originated during this phase as reactions to the release of the internal stresses inherited from the earlier phases of the intrusive.

### The post-intrusion phase I

In Table 4, the time limits to the post-intrusion phase I have been established largely on the basis of absolute age determinations by O. Kouvo (see Gaál and Rauhamäki, 1971). The determinations indicate that this phase came to an end 1800

TABLE 4  
Structural elements, their relative ages and the respective geological phases.

The phases of the intrusive	Tensional and compressional structures inside the intrusive	Structures of the metamorphic rocks outside the intrusive	Regional phases	Age Ma
Pre-intrusion phase		Bedding cleavage (S <sub>1</sub> )	Sedimentation, onset of metamorphism	
Intrusion	Mineral lineations The ringshaped pattern of gently dipping fracturing The radial pattern of steeply dipping fracturing	Gently plunging axes and lineations (F <sub>1</sub> ), schistosity (S <sub>2</sub> )	Progressive metamorphism First deformation	1950
Post intrusion phase I  Fragmentation Local metamorphism	Protoclastic mylonites and ultramylonites Mafic dykes Felsic dykes Composite dykes Slip cleavage	Schistosity (S <sub>3</sub> ) Steeply plunging axes and lineations (F <sub>2</sub> ) Thrust and wrench structures (F <sub>3</sub> ) Crenulation cleavage (S <sub>4</sub> )	Peak of metamorphism, main deformation  Regression of metamorphism	1925
Post intrusion phase II Minor faulting & fracturing, local metamorphism	Mylonites Slip cleavage, striations Felsic dykes	Crenulation cleavage (S <sub>5</sub> )	Local regressive metamorphism	1800

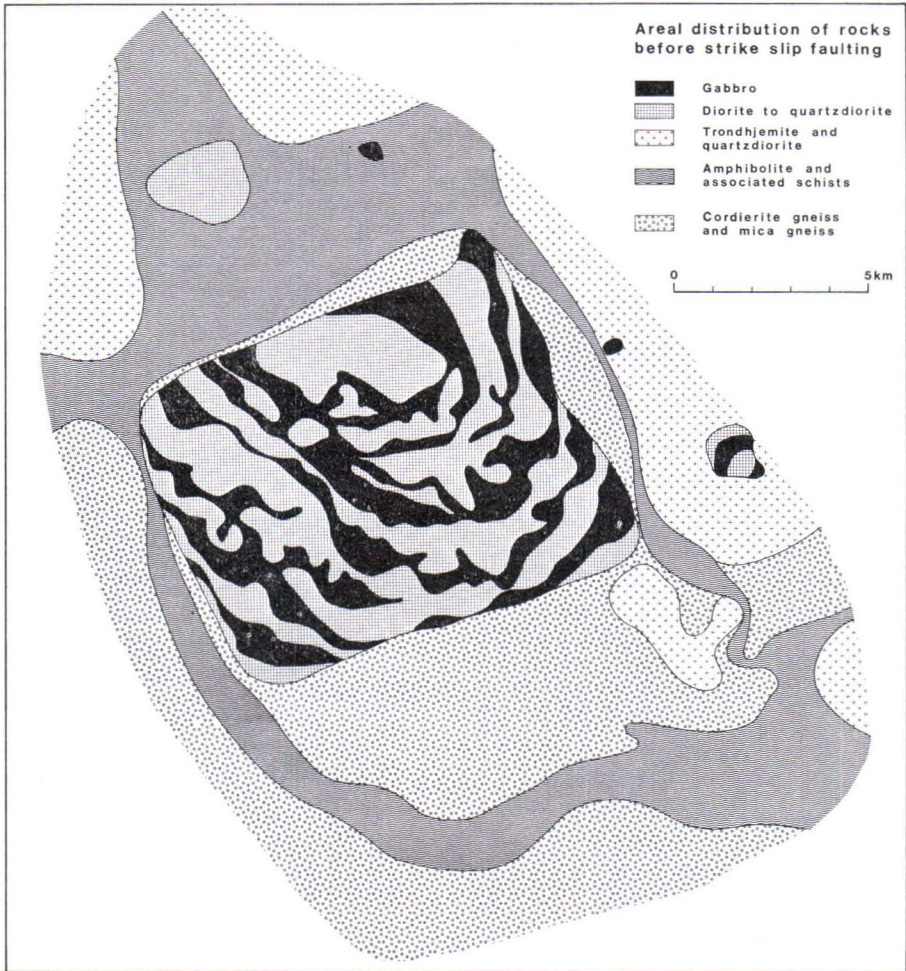


FIG. 40. Areal distribution of rocks before the hypothetical strike slip faulting.

Ma ago, which is the age of the post-tectonic intrusive rocks in the bedrock of Finland. The beginning of this phase can be dated to 1925 Ma, which is about the age of Svecof Karelian intrusives and the age of certain hypersthene-bearing rocks in the northern Haukivesi area. This dating marks the probable end of the intrusion phase of the Joutsenmäki mafic body.

Most of the significant deformational structures of the intrusive and the regional structures shared by the intrusive and the rocks around it originated during this phase. The relatively competent intrusive body broke into a breccia, whereas the less competent supracrustal formations and migmatites reacted in a more plastic way. The porphyric granodiorite of the migmatite zone (p. 7—15) was probably formed as a reaction to the most intensive deformation in the contacts between the intrusive

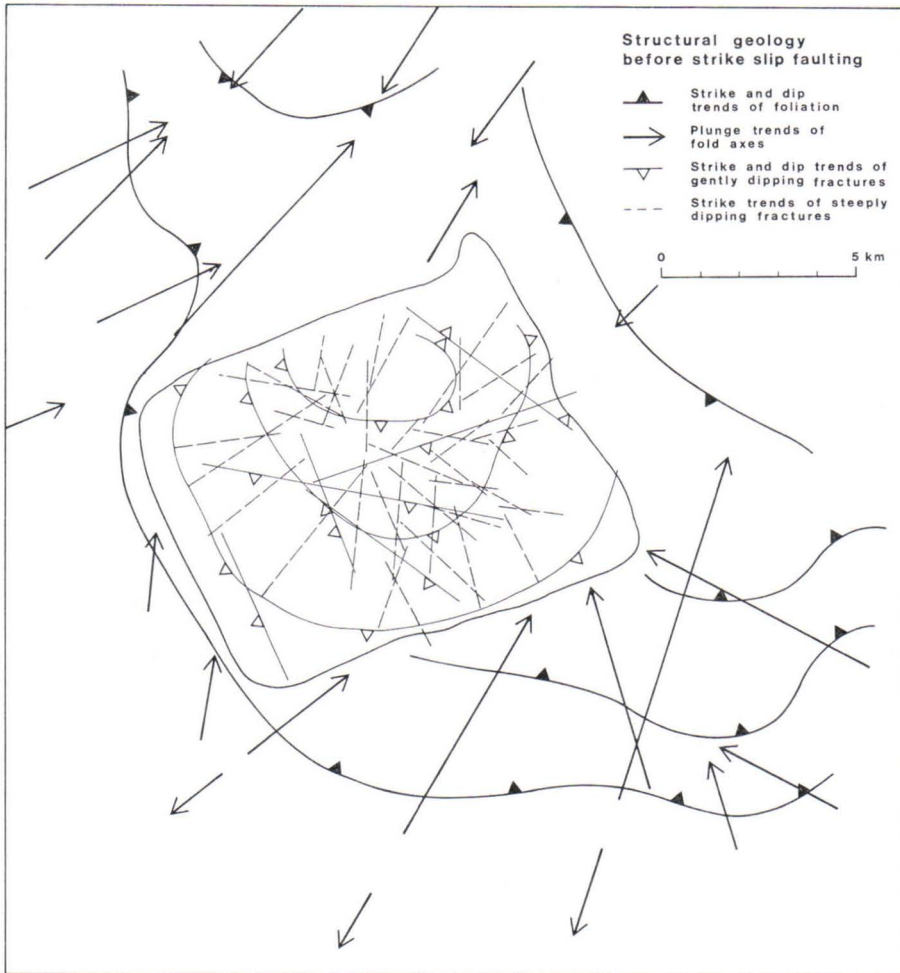


FIG. 41. Structural features of the intrusive and its surroundings before the strike slip faulting.

body and the surrounding supracrustal rocks. The primary reason for the deformation may have been the fact that high stresses concentrated near the sill termination, thereby inducing permanent deformation (see Johnson and Pollard, 1973). Thus, porphyric granodiorite is considered as a late-metamorphic rock, possibly a kind of blastomylonite (see Higgins, 1971).

One is tempted to reconstruct the geological situation preceding the major fragmentation of the intrusive by the regular network of shear zones (Fig. 25), lineaments (Figs. 22 and 23), inferred fault zones (Figs. 29–33), and the rather simple strike-frequency distribution patterns of the structural elements of the southern Haukivesi area. The analyses indicate that the movements responsible were (1) strike

slip faults, (2) normal faults, (3) minor thrust and reverse faults. Certain generations of fractures and foliation can be attributed to these movements (Table 4).

Following the fault lines and relying on the tectonic marker horizon in Fig. 29, the reconstruction was executed step by step for the various geological maps in Figs. 2 and 6—25 according to the following rules: (1) The most recent transcurrent faults were dextral in the direction  $335^\circ$  and the overall separation within the intrusive was about 2.5 km. (2) At the same time or somewhat earlier there was dextral strike slip faulting in the direction  $305^\circ$ . The separation within the southern Haukivesi area was about 12 km. (3) Slightly before the forementioned, sinistral strike slip faulting occurred in the direction  $070^\circ$ . The separation is not known. For the reconstruction a separation of 1 km is postulated for the fault zone adjoining the southern contact of the intrusive.

The effects of vertical and thrust faulting had to be omitted, since the separations are not known, but some information about them can be inferred from the maps in Figs. 27 and 28. After the reconstruction procedure, the central parts of the area, especially the intrusive area, could be established more reliably than the marginal parts.

The map of the areal distribution of the rocks before strike slip faulting (Fig. 40) shows a quadratic or rounded mafic body surrounded by cordierite gneiss and amphibolite. According to the structural map (Fig. 41) and the general stratigraphical hypotheses by Gaál and Rauhamäki (1971, p. 6—7), the intrusive rests on a cordierite-gneiss (turbidite) formation overlying a bed of amphibolite (volcanics). The intrusive is located in a syncline deepening towards the southeast, which is either relatively simple or possibly has an up-domed core as indicated in the cross-sections (Figs. 27 and 28). The other mafic bodies of the area may be fragments of the same formation, which floated like a thin sill or laccolith in the schists. The trondhjemite bodies, possibly sills, locally overlie the cordierite gneiss but the majority tectonically underlie the amphibolite.

The borders of the intrusive in Fig. 40 are sublinear. This may be because of dip slip faults during the downwarping of the intrusive during or before the strike slip faulting. Such movements tend to resemble the caldera-like subsidence typical of ring complexes as reported by Budanov (1970).

The distribution of gabbro and diorite inside the intrusive has a zonal character. When completed, the zones would presumably form ellipses lying one inside the other and conforming to the design of the above syncline.

One group of mineral lineations inside the intrusive may have formed in the direction of flow and another group normal to it. These groups have been tentatively separated in Fig. 42. Several lineations plunge towards the borders of the intrusive, thereby indicating that either the marginal parts of the intrusive are bend down or that the primary flow was downwards.

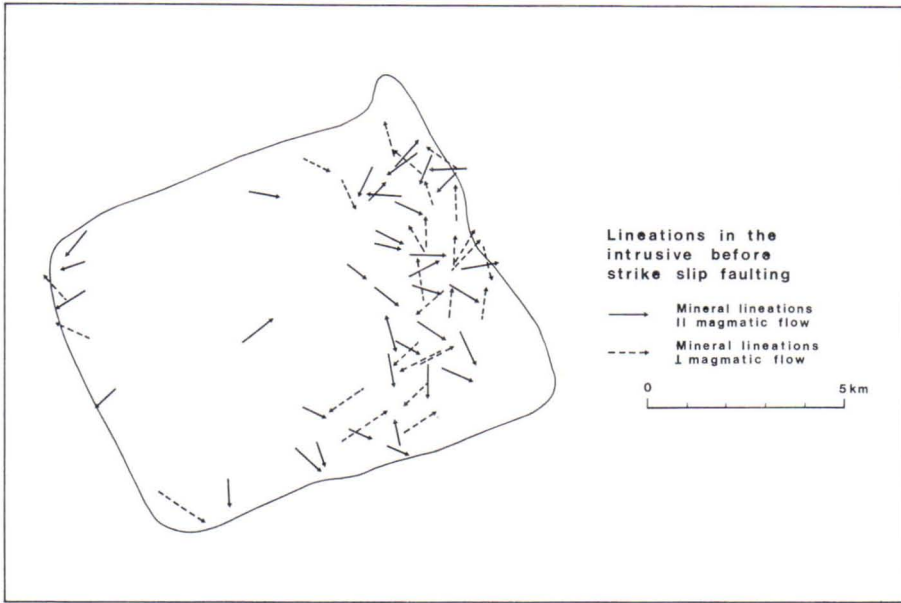


FIG. 42. Mineral lineations in the intrusive before the strike slip faulting.

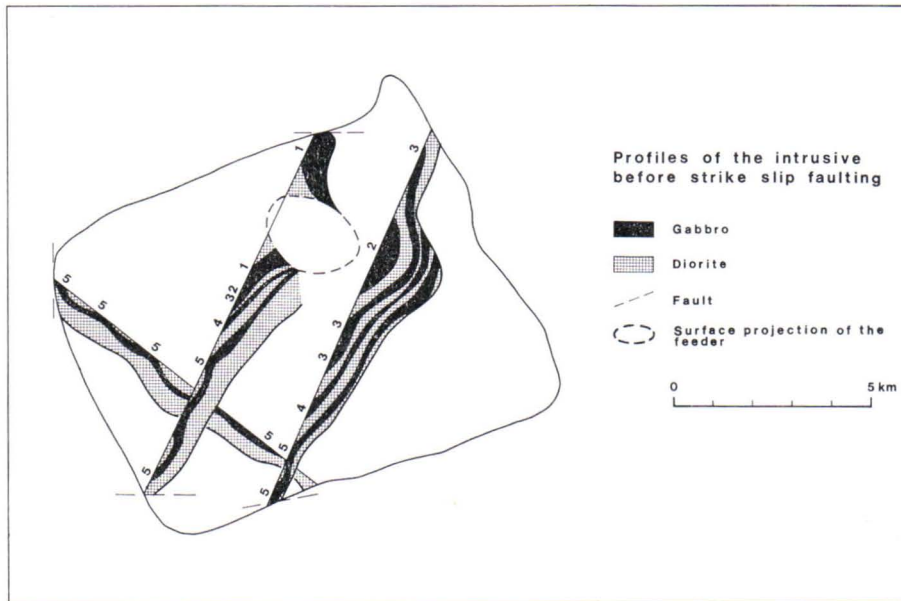


FIG. 43 Profiles of the intrusive before the strike slip faulting. The numbers refer to the possible layers as counted from the hypothetical feeder towards the margins.

The gently dipping fractures of the intrusive dip towards the borders and also appear in linear zones across the intrusive. Vertical fractures extend radially from the core towards the borders.

No zonal arrangement of vertical fractures is visible after completion of the reconstruction procedure. In Fig. 41 both the fractures following regional trends and those conforming to the contact directions are omitted; the latter are shown in Fig. 43.

The strain and stress analysis suggests that the regional schistosity, oriented east to west, and the steeply plunging lineations and fold axes around the intrusive can be attributed to wrench faulting simultaneous with the above faulting of the intrusive (model III A and B, Fig. 39). In the reconstruction, structures in an east to west direction do not show any striking continuities, but rather the postulated primary compression directions,  $340^\circ$  and  $035^\circ$ , seem to show up much better than before the reconstruction. They are also major axial directions together with  $305^\circ$  and  $070^\circ$ . Geological contacts also give the direction  $070^\circ$ , possibly because the reconstruction was not completed.

The most questionable feature in the reconstruction is the pattern exhibited by the fold axes, and especially by the axial trends in the direction  $035^\circ$ . According to the strain and stress analysis, these trends can be attributed to thrust movements towards south-southwest (Fig. 39, model IC) either as primary trends or as results of the refolding of earlier folds, e.g. those with steeply plunging axes (*cf.*, p. 19). Thus, certain axial trends of Fig. 41 may be subsequent to or contemporaneous with the strike slip faulting during the post intrusion phase I. However, the four directions,  $305^\circ$ ,  $335\text{--}340^\circ$ ,  $035^\circ$  and  $070^\circ$ , are still the most important directions during the intrusion phase.

### The intrusion phase

The zonality of the intrusive indicates that the original magma channel ran close to the northern border. The zonality may be due to successive intrusions through the same channel. It is the point of the absolute maximum of 35 mgal on the Bouguer anomaly map by Honkasalo (1962).

The intrusion phase can be dated in several ways:

(1) Absolute age determinations of the Svecokarelian bedrock have dated a generation of mafic intrusives or associated intermediate and felsic bodies to 1920—1950 Ma. However, owing to the paucity of these determinations, they are not necessarily valid in every case.

(2) Most of the structural features of the southern Haukivesi area can be attributed to the post-intrusive movements described above; the effects of the pre-intrusive movements are rather modest. According to the reconstructions, it seems that the

Joutsenmäki mafic body intruded during the gentle folding of the supracrustal beds, the folding imparting it the primary form of an elliptical pancake. This indicates that, either the latest movements totally deformed the earlier structures, or that there were not many regionally conspicuous structural features to be deformed. If the latter is true, the intrusion phase should be dated to around the earliest phases of major regional movements.

(3) It may be inferred from the rather homogeneous, even texture of the intrusive, the fine-grained inclusions (p. 7), the faint remnants of possible magmatic flow and the rather coarse-featured, weakly differentiated layered structure exhibited by the gabbro and diorite zones that, at the time of the intrusion, the mafic body was relatively hot and viscous and that it solidified relatively rapidly. The scarcity of flow structures might be due to the plug flow of a Bingham magma (see Johnson and Pollard, 1973). This means that the central portion of Bingham magma flows as a rigid body. If this is the case, the intrusive would be the central portion of a far greater massif.

There are no obvious indications of an intrusive contact between the intrusive and the surrounding metamorphic rocks (p. 12). This and the assumed blastomylonitic migmatite zone around the intrusive (p. 51) can be taken as proofs of the allochthonous nature of the intrusive (*cf.* Burch, 1968). On the other hand, the reconstructions indicate that the primary structure of the intrusive is still traceable; hence the major tectonic transport of the intrusive did not necessarily take place en block. The intrusive can still be considered as an autochthonous body, even though it has been broken into pieces and some of the pieces moved apart. In any event, the body probably intruded prior to the peak of the latest regional metamorphism that — together with the tectonic agency — was able to destroy the immediate effects of the hot intrusion on the weakly metamorphosed sedimentary pile. The contact reactions may have been faint owing to the relative thinness of the primary sill or laccolith. It is also possible that the lack of reaction products is due to the fact that we are now dealing only with the footwall contact of the intrusive. The first intrusion phase may have produced a thin but protective shell against the wall rock.

Thus, the timing of the intrusion phase is problematic. In this study, it is concluded that the mafic body is a result of several successive hot intrusions that expanded laterally between the sedimentary piles to form a sill or laccolith during the early phase of the progressive regional metamorphism.

The intrusion phase gave birth to the petrographical zoning of the mafic body, to the mineral lineations and also to certain fracture patterns. The ring-shaped fractures dipping gently outwards can be considered as a reaction between the consolidating, expanding mafic mass and the surrounding rocks (Fig. 44). The radial fractures may reflect the first rapid cooling phase of the laccolith. As a consequence of the primary stresses of the cooling intrusive these old structural trends very probably became more prominent during later movements.



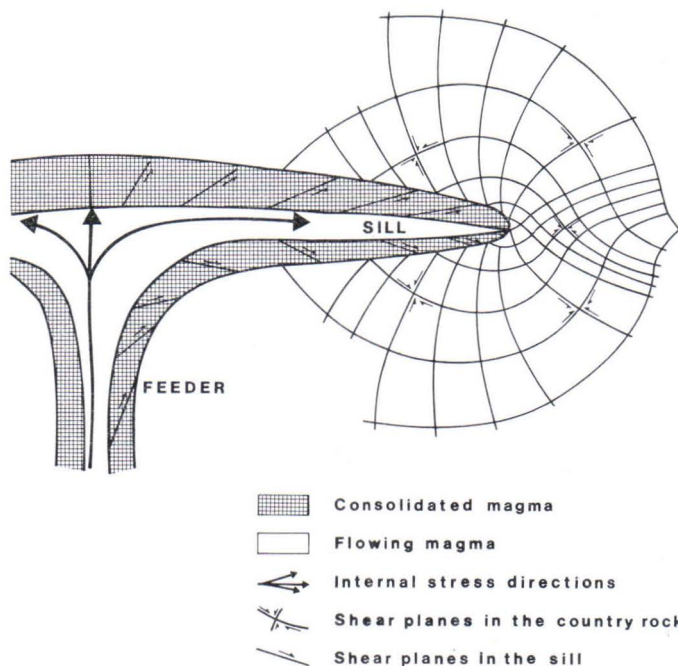


FIG. 44. A model to explain the possible relationship between certain structural features and the intrusion mechanism of the Joutsenmäki mafic body. Modified after Pollard and Johnson (1973).

### The mechanism of intrusion

According to Johnson and Pollard (1973), the most significant types of mechanism that can contribute to magma driving pressure are (1) the density contrast between the magma and the surrounding country rock, (2) tectonic events, such as pervasive folding, and (3) fluids dissolved in the magma or present in the pores of the country rock.

At depth, the density contrast might have been the most significant mechanism, but close to the level of the intrusion its influence would probably have ceased to operate because there is no marked contrast between the density of the intrusive (2.9–3.0) and the densities of the country rocks (2.7–3.0). The effect of dissolved fluids is not known well enough, and hence the discussion centres around the tectonic factor.

The reconstructed models indicate that the primary intrusive possibly solidified in a syncline close to a minor unconformity in the sedimentary strata marked by conglomerates (Gaál and Rauhamäki, 1971). This may have been a major factor controlling the shape and size of the mafic body as shown in Figs. 40 and 43.

Since the original size and roof of the intrusive are not known, it is impossible to determine whether the body is actually a sill or a laccolith. According to Pollard and Johnson (1973), these both form a sequence of growth whereby, after spreading over a distance some three times the effective thickness of the overburden, the overlying layers begin to bend significantly upwards; this stage marks the transition from a sill to a laccolithic intrusion. The syncline mentioned above might also be a result of the thickening and bending of the intrusive. In Fig. 44 the internal fracture pattern of the intrusive is related to the hypothetical sequence of growth of the primary sill.

According to Mudge (1968), a depth of 7 500 ft. may be about the deepest level at which magma pressure can exceed lithostatic pressure, and thus, at which a sill can be injected. Pollard and Johnson (1973) reject this limitation because magma pressure should exceed lithostatic pressure the whole way to the source. Thus, pressure does not impose a lower limit on sill formation.

## CONCLUSIONS

Solutions can now be given to the problems stated in the introduction.

(1) Certain fractures dipping gently outwards as well as radial, steeply dipping fractures originated as an immediate response to the intrusion phase(s) of the Joutsenmäki mafic body. These fractures can be called the internal fracture pattern of the body. The strikes of the gently dipping fractures locally conform to the primary petrographic zoning of the intrusive but, in principle, the internal fracture pattern crosses the petrographic structures.

(2) The internal fracture pattern is not necessarily in straight geometrical relationship to the structural patterns of the surroundings of the intrusive. Exceptions to this are the features caused by the sedimentary and tectonic structures prevailing during the intrusion phase. However, most of the fracturing that originated during the post-intrusion phases conforms to the general regional tectonics and can be called the external fracture pattern of the intrusive.

(3) The history of the mafic body can be followed step by step back to the intrusion phase with the aid of fracture analytics. Certain regional processes like transcurrent faulting can also be characterized and verified. After covering the fracture generations originated during the post-intrusion phases, the major structural trends that dominated during or before the intrusion phase are still visible. The extent of the regional information gained is, however, rather limited both in time and space because it concerns only the rocks in the immediate surroundings of the intrusive. These belong, according to Gaál and Rauhamäki (1971), to a turbidite sequence deposited on eugeosynclinal rocks.

In the treatment of the data, six or eight regional directional maxima of lineaments were recognized. Most of the largest ones, the class I lineaments, were pre-

sumed to mark complex fault zones, some characteristics of which were discussed. The same directional and fault trends were found to exist in the structural patterns of the intrusive and its vicinity. These findings may justify some further conclusions: The intrusion took place before major regional movements. When the original sill or laccolith was broken, some of the pieces were separated. The intrusion was controlled by an older structural pattern which also determined the major paths followed by the post-intrusion deformation. Thus, the external fracture pattern of an intrusive, analogical to the Joutsenmäki mafic body, may be used as a tool in the analysis and characterization of the course of tectonic events in the surroundings of that intrusive.

#### ACKNOWLEDGMENTS

Outokumpu Oy permitted the bulk of the investigation to be carried out with the help of the facilities of the company's Exploration Department. Valuable help during the field work was given by Mr. Erkki Viluksela, Dr. Gabor Gaál and Mr. Tapio Karppanen. Professor Heikki V. Tuominen of the University of Helsinki was always ready with his friendly advice. Discussions with Dr. Aulis Häkli and Messrs. Jussi Aarnisalo, Kalevi Korsman and Seppo Lavikainen proved very fruitful.

The manuscript was critically read by Professor Aimo Mikkola and Dr. Gabor Gaál.

Mrs. Gillian Häkli corrected the language of the author's English manuscript.

The publication of the study in the Bulletin series of the Geological Survey of Finland was arranged by Professor Herman Stigzelius, Director of the Survey.

To all these and to several other persons not mentioned here, I wish to express my sincere gratitude.

Financial support was provided by a grant awarded by the Foundation of Outokumpu Oy.

## REFERENCES

- BALK, R. (1948) Structural behaviour of igneous rocks. Edwards Brothers, Inc. Ann Arbor, Michigan.
- BELL, T. H. & ETHERIDGE, M. A. (1973) Microstructure of mylonites and their descriptive terminology. *Lithos* 6, 337—48.
- BERGER, A. R. and PITCHER, W. S. (1970) Structures in granitic rocks: A commentary and critique on granite tectonics. *Proc. Geologists' Association* 81, 441—461.
- BROWN, R. L. and HELMSTAEDT, H. (1970) Deformation history in part of the Lübeck-Belkisle zone of southern New Brunswick. *Can. J. Earth Sci.* 7, 748—767.
- BUDANOV, V. I. (1970) Mechanism of formation of ring complexes. *Doklady Acad. Sci. U.S.S.R., Earth Sci. Sect.*, 191, 59—62.
- BURCH, S. H. (1968): Tectonic emplacement of the Burro Mountain Ultramafic Body, Santa Lucia Range, California. *Geol. Soc. Amer. Bull.* 79, 527—544.
- CROSBY, G. W. and LINK, P. K. (1972) Stress reorientation during folding. *Geol. Rundschau* 61, 413—429.
- DIETERICH, J. H. (1969): Origin of cleavage in folded rocks. *Amer. J. Sci.* 267, 155—165.
- ESCHER, A. and WATTERSON, J. (1974) Stretching fabrics, folds and crustal shortening. *Tectonophysics* 22, 223—231.
- FLINN, D. (1965) On the symmetry principle and the deformation ellipsoid. *Geol. Mag.* 102, 36—45.
- GAÁL, G. (1972) Tectonic control of some Ni-Cu deposits in Finland. 24th IGC, Sect. 4, 215—224.
- »— and RAUHAMÄKI, E. (1971) Petrological and structural analysis of the Haukivesi area between Varkaus and Savonlinna, Finland. *Bull. Geol. Soc. Finland* 43, 265—337.
- GAY, S. P. (1972) Fundamental characteristics of aeromagnetic lineaments. Their geological significance, and their significance to geology. *Amer. Stereo Map Co. Techn. Publ.* 1, 1—94.
- HACKMAN, V. (1933) Kivilajikartan selitys. Lehti D2 Savonlinna. Suomen Geologinen yleiskartta [General Geological Map of Finland]. Suomen Geologinen toimikunta, 1—175.
- HÄKLI, T. A. (1971) Silicate nickel and its application to the exploration of nickel ores. *Bull. Geol. Soc. Finland* 43, 247—263.
- HAMAN, P. J. (1961) Lineament analysis on aerial photographs. *West Can. Research Publ.*, P.O. Box 997, Calgary, Alberta, 2 (1), 1—29.
- »— (1964) Geomechanics applied to fracture analysis of aerial photographs. *West Can. Research Publ.*, P.O. Box 997, Calgary, Alberta, 2 (2), 1—84.
- HANCOCK, P. L. (1972) The analysis of en echelon veins. *Geol. Mag.* 109, 269—276.
- HÄRME, M. (1961) On the fault lines in Finland. *C.R. Soc. Geol. Finlande* 33, 437—444.
- HIETANEN, A. (1967) On the facies series in various types of metamorphism. *J. Geol.* 75, 187—214.
- HIGGINS, M. W. (1971) Cataclastic rocks. *U.S. Geol. Surv. Prof. Paper* 687. 1—97.
- HOBBS, W. H. (1911) Repeating patterns in the relief and in the structure of land. *Geol. Soc. Amer. Bull.* 22, 123—126.
- HONKASALO, T. (1962) Gravity survey of Finland in the years 1945—1960. Bouguer anomalies. *Finnish Geod. Inst. Publ.* 55.
- JAEGER, J. C. and ROSENGREN, K. J. (1969) Friction and sliding of joints. *Proc. Aust. Inst. Min. Met.* 229, 93—104.

- JOHNSON, A. M. and POLLARD, D. D. (1973) Mechanics of growth of some laccolithic intrusions in the Henry Mountains, Utah. *Tectonophysics* 18, 261—309.
- JOHNSON, M. R. W. (1967) Mylonite zones and mylonite banding. *Nature* 213 (5 073), 246—247.
- KAZANSKY, V. I. (1972) Dislocation metamorphism and endogenous ore formation in fault zones in crystalline basement. 24th IGC, Sect. 4, 482—487.
- KORSMAN, K. (1973) Sheet 3233, Rantasalmi. Geological Map of Finland. Geol. Surv. of Finland.
- LAJTAI, E. Z. (1968) Brittle fracture in direct shear and the development of second order faults and tension gashes. *Geol. Surv. Canada, Paper* 68—52, 96—100.
- »— & LAJTAI, V. N. (1974) The evolution of brittle fracture in rocks. *J. Geol. Soc. Lond.* 130, 1—18.
- LATTMAN, L. H. (1958) Technique of mapping geologic fracture traces and lineaments on aerial photographs. *Photogr. Engng.* 24, 568—576.
- MEANS, W. D. and WILLIAMS, P. F. (1972) Crenulation cleavage and faulting in an artificial salt mica schist. *J. Geol.* 80, 569—591.
- MIKKOLA, A. and NIINI, H. (1968) Structural position of the ore bearing areas in Finland. *Bull. Geol. Soc. Finland* 40, 17—33.
- »— and VUORELA, P. (1973) Ore bearing areas and linearity in Finnish bedrock [Abstract]. XI Nordiska geologiska vintermötet Oulu/Uleåborg, 1974. B, 71—72.
- MIYASHIRO, A. (1973) *Metamorphism and metamorphic belts*. G. Allen & Unwin, London.
- MOGI, K. (1973) Rock fracture. *Ann. Rev. Earth Planet. Sci.* 1, 63—84.
- MUDGE, M. R. (1968) Depth control of some concordant intrusions. *Geol. Soc. Amer. Bull.* 79, 315—332.
- NICOLAS, A., BOUDIER, F. and BOULLIER, A. M. (1973) Mechanisms of flow in naturally and experimentally deformed peridotites. *Amer. J. Sci.* 273, 853—876.
- PARKKINEN, J. (1971) Joutsenmäen-Tolvanniemen gabrodioriittimassiivi. *Manuscr., Arch. Geol. Min., Univ. Helsinki.*
- PETROV, A. J. (1970) Old faults in the eastern part of the Baltic Shield. *Doklady Acad. Sci. U.S.S.R., Earth Sci. Sect.*, 191, 56—62.
- PITCHER, W. S. and BERGER, A. R. (1972) *The geology of Donegal*. Wiley Interscience, N.Y., London, Sydney, Toronto.
- POLLARD, D. D. and JOHNSON, A. M. (1973) Mechanics of growth of some laccolithic intrusions in the Henry Mountains, Utah, II. *Tectonophysics* 18, 311—354.
- PRICE, N. J. (1966) Fault and joint development in brittle and semi-brittle rock. Pergamon, London.
- »— (1968) A dynamic mechanism for the development of second order faults. *Geol. Surv. Canada, Paper* 68—52, 49—78.
- RAMSAY, J. G. (1967) *Folding and fracturing of rocks*. McGraw-Hill Book Co., U.S.A.
- »— and GRAHAM, R. H. (1970) Strain variation in shear belts. *Can. J. Earth Sci.* 7, 786—813.
- SALTIKOFF, B. (1965) Pohjois-Säämingin (Varparannan) intrusiivimassiivi ja sen ympäristö. *Manuscr., Arch. Geol. Min., Univ. Helsinki.*
- SCHWERTNER, W. M. (1973) Schistosity and penetrative mineral lineation as indicators of paleostrain directions. *Can. J. Earth Sci.* 10, 1233.
- SÖDERHOLM, B. (1970) Frekvensanalys av skiffrighetsstrykningarna i Finlands berggrund. *Manuscr., Arch. Geol. Min., Univ. Helsinki.*
- TALVITIE, J. (1971) Seismotectonics of the Kuopio region, Finland. *Bull. Comm. Géol. Finlande* 248, 41 p.
- TCHALENKO, J. S. (1970) Similarities between shear zones of different magnitudes. *Geol. Soc. Amer. Bull.* 81, 1625—1640.
- TUOMINEN, H. V., AARNISALO, J. and SÖDERHOLM, B. (1973) Tectonic patterns in the central Baltic shield. *Bull. Geol. Soc. Finland* 45, 205—217.

- TURNER, F. J. & VERHOOGEN, J. (1960) *Igneous and metamorphic petrology*. McGraw-Hill Book Co. Inc., N.Y.
- WILCOX, R. E., HARDING, T. P. and SEELY, D. R. (1973) Basic wrench tectonics. *Amer. Assoc. Petr. Geol. Bull.* 57, 74—96.
- WINKLER, H. G. F. (1970) Abolition of metamorphic facies. *Neues Jahrbuch für Mineralogie, Mh.* 5, 189—248.
- WOOD, D. S. (1974) Current views of the development of slaty cleavage. *Ann. Rev. Earth Planet. Sci.* 2, 369—401.









